UNIVERSITÄT ZU LÜBECK
INSTITUT FÜR MATHEMATIK

Host-parasite coevolution with multiple types

Wirt-Parasit-Coevolution mit mehreren Typen

Masterarbeit

im Rahmen des Studiengangs
Mathematik in Medizin und Lebenswissenschaften
der Universität zu Lübeck

vorgelegt von
Hanna Schenk

ausgegeben und betreut von
Prof. Dr. Arne Traulsen

mit Unterstützung von
Dr. Chaitanya S. Gokhale

Die Masterarbeit ist im Rahmen einer Tätigkeit in der Abteilung Evolutionstheorie des Max-Planck-Instituts für Evolutionsbiologie in Plön entstanden.

Lübeck, den 25. August 2015

Eidesstattliche Erklärung

Ich versichere an Eides statt, die vorliegende Arbeit selbstständig und nur unter Benutzung der angegebenen Hilfsmittel angefertigt zu haben.

Lübeck, den 25. August 2015

Abstract

The coevolution of hosts and parasites has been analysed most prominently with two types using deterministic, population-based models. These models usually generate oscillatory (Red Queen) dynamics. So far it was unclear in which way Red Queen dynamics persists with more than two types of hosts and parasites. In stochastic models changing population size reduces the probability of Red Queen dynamics in a model with two types. It was also argued that with more types in a stochastic model Red Queen dynamics can be observed in a limited parameter space which decreases as the number of host and parasite types increases. In this thesis an arbitrary number of types is examined using deterministic methods. A fixed point and stability analysis is conducted and constants of motions are formulated. We show that Red Queen dynamics can still exist. However, Hamiltonian chaos is possible in large areas of the parameter space.

Zusammenfassung

Die Koevolution von Wirten und Parasiten wird meist mit zwei Arten mittels deterministischen, populationsbasierten Modellen analysiert. Diese Modelle erzeugen in der Regel oszillierende (Red Queen) Dynamiken. Bisher war unklar, in welcher Weise Red Queen Dynamiken bei mehr als zwei Arten von Wirten und Parasiten bestehen bleiben. In stochastischen Modellen reduziert eine veränderliche Populationsgröße die Wahrscheinlichkeit von Red Queen Dynamik in einem Modell mit zwei Arten. Es wurde außerdem diskutiert, dass mit mehr Arten in einem stochastischen Modell Red Queen Dynamik in einem begrenzten Parameteraum besteht. Dieser Parameterraum reduziert sich, je höher die Anzahl der Wirt und Parasit Typen. In dieser Arbeit wird, unter Verwendung von deterministischen Methoden, eine beliebige Anzahl an Arten von Wirten und Parasiten untersucht. Eine Fixpunkt- und Stabilitätsanalyse wird durchgeführt und Bewegungskonstanten werden formuliert. Wir zeigen, dass Red Queen Dynamik noch existiert. Jedoch entsteht in großen Bereichen des Parameterraums Hamilton'sches Chaos.

Acknowledgements

I would like to thank Prof. Dr. Arne Traulsen for having included me into his research group, inspired me for this interesting project and having guided me throughout the last six months.

Additionally, I want to thank Prof. Dr. Andreas Rößler for his willingness to evaluate my thesis.

Furthermore, I want to express my gratitude towards Dr. Chaitanya S. Gokhale for his advise not only regarding contents but also on technical and organisational aspects.

I also want to thank the Evolutionary Theory group at the Max Planck Institute Plön for making me feel welcome from the very beginning, helping me with whatever problem came up and inviting me to all the delightful group activities.

Contents

1 Introduction

Parasitism is everywhere, whether in human disease (malaria, leishmania, cercarial dermatitis), in plants [Coors et al., 2008] or in the impact on allergies [Bell, 1996]. The importance of parasites must not be underestimated and should be incorporated into models on evolution. Because of the often deadly selective pressure from parasites, resistant hosts have been able to evolve which in turn selects for certain parasites. The coevolution of host and parasite is therefore a contemporary topic.
Theories of host-parasite coevolution propose explanations for phenomena such as the evolution of sexual reproduction [Lively, 2010; Hamilton et al., 1990]. Here it is believed that increased diversity compensates for the otherwise twofold loss of fitness. In general it is necessary to study not only evolutionary models but especially coevolutionary models which lead to different results [Best et al., 2009].

Mathematical models simplify and conceptualise biological contexts. This can give a broad overview of the topic but it can also lead to new ideas and perspectives on the topic. Models can give insight into the long-term future which is difficult to reproduce in the lab or observe in nature for many generations. Models can predict the future or in the case of evolution also infer the past [Lambert, 2014]. Theoretical models for host-parasite coevolution often include the matching allele (MA) model or the gene-for-gene (GfG) model [Flor, 1955; Engelstädter, 2015; Agrawal and Lively, 2002]. In the MA model only parasites with two identical alleles can infect the corresponding host type. In the GfG model each allele contributes to the infectiousness of the parasites, so that some can infect multiple hosts. Host-parasite coevolution is believed to follow Red Queen dynamics [van Valen, 1973] a metaphor derived from the Red Queen's words to Alice in *Through the looking glass*: "it takes all the running *you* can do, to keep in the same place" [Carroll, 1871]. Red Queen dynamics suggest a negative frequency-dependent selection of host and parasite resulting in oscillating frequencies. The Red Queen hypothesis has been strengthened by empirical results from pond sediments [Decaestecker et al., 2007] and freshwater snails [Koskella and Lively, 2009]. It remains to be investigated under which circumstances the Red Queen persists [Salathé et al., 2008].

A system with constant population sizes for hosts and parasites has been analysed with replicator dynamics. Changing population sizes were recently combined in a Lotka-Volterra model [Song et al., 2015]. Here, the matching allele model and the gene-for-gene model were incorporated into the fitness effect. Adding stochasticity to the Lotka-Volterra dynamics leads to extinction of species, halting Red Queen dynamics [Gokhale et al., 2013]. So far two types of hosts and two types of parasites were considered. Building on this we analyse multiple types of hosts and parasites with replicator dynamics and Lotka-Volterra dynamics. Although a replicator dynamics system with n types can be transformed into a Lotka-Volterra system with $n-1$ types for a single species system it is nevertheless necessary to look at both models in a multispecies system since the assumptions do not allow such a transformation. Different models (MA, GfG or other interactions) are realised using diverse (and preferably most general) payoff matrices. Both approaches are mathematically described by a system of ordinary differential equations, which are solved numerically. Analytically, a stability analysis is conducted and constants of motions for several models are presented. We will also show that the system can already become chaotic in a certain parameter space for a minimum of three hosts and parasites in a most simple matching allele replicator dynamics model.

2 Mathematical methods

The two approaches used in this thesis are based on systems of ordinary differential equations. With increasing number of dimensions systems of ordinary differential equations become harder to solve explicitly. It is therefore necessary to use other methods to analyse the biological system. For each model fixed points and their stability and constants of motion will be investigated. Chaos is analysed with Lyapunov exponents which give insight into the sensitivity of initial conditions. Before elaborating these methods, the interaction models are introduced.

2.1 Interaction models

Fitness effects of parasites on host and vice-versa are collected in a matrix, which intuitively describes the influence of the different types of one species on the different types of the other species. Assuming n types of hosts and n types of parasites, $M^H \in \mathbb{R}^{n\times n}$ describes the loss of fitness hosts suffer from specific parasite types, $M^P \in \mathbb{R}^{n\times n}$ denotes the parasites' gain. For example $\left(M^H\right)_{2,4}$ is the fitness effect that parasite type 4 has on host type 2.

2.1.1 Matching allele model

To introduce host parasite dynamics it is best to look at the simple matching allele model where only matching host and parasite can directly interact with each other. This model can be described by the following payoff matrices

$$M^H = \begin{pmatrix} -1 & 0 & \cdots & 0 \\ 0 & -1 & \cdots & 0 \\ \vdots & \vdots & \ddots & \vdots \\ 0 & 0 & \cdots & -1 \end{pmatrix} \qquad \text{and} \qquad M^P = \begin{pmatrix} 1 & 0 & \cdots & 0 \\ 0 & 1 & \cdots & 0 \\ \vdots & \vdots & \ddots & \vdots \\ 0 & 0 & \cdots & 1 \end{pmatrix}. \tag{2.1}$$

2.1.2 Cross-infection

Assuming that neighbouring parasite types have similar infection patterns and thus have the same negative fitness effect on a host, the following model is constructed. Each host can now be infected by three parasite types of which one can infect two other hosts and two can each infect one other host. On the other hand a parasite type can benefit from three different host types. One could say that neighbouring hosts h_i and $h_{i\pm1}$ have similar genetic material or are similar in phenotype and therefore can be infected by similar parasites p_i and $p_{i\pm1}$. For symmetry reasons types 1 and n can also interact with three types of the other species.

$$M^H = \begin{pmatrix} -1 & -1 & 0 & 0 & \cdots & -1 \\ -1 & -1 & -1 & 0 & \cdots & 0 \\ 0 & -1 & -1 & -1 & \cdots & 0 \\ \vdots & \vdots & \ddots & \ddots & \ddots & \vdots \\ 0 & 0 & \cdots & -1 & -1 & -1 \\ -1 & 0 & \cdots & 0 & -1 & -1 \end{pmatrix} \qquad M^P = \begin{pmatrix} 1 & 1 & 0 & 0 & \cdots & 1 \\ 1 & 1 & 1 & 0 & \cdots & 0 \\ 0 & 1 & 1 & 1 & \cdots & 0 \\ \vdots & \vdots & \ddots & \ddots & \ddots & \vdots \\ 0 & 0 & \cdots & 1 & 1 & 1 \\ 1 & 0 & \cdots & 0 & 1 & 1 \end{pmatrix} \tag{2.2}$$

2.1.3 General infection

A most general model is now drawn: A circulant matrix where every diagonal has a specific value [Hershey and Rao Yarlagadda, 1986]. We will see later that some further assumptions need to be made in order to construct a constant of motion.

$$M^H = \begin{pmatrix} \alpha_1^P & \alpha_2^P & \cdots & \alpha_{n-1}^P & \alpha_n^P \\ \alpha_n^P & \alpha_1^P & \alpha_2^P & & \alpha_{n-1}^P \\ \vdots & \alpha_n^P & \alpha_1^P & \ddots & \vdots \\ \alpha_3^P & & \ddots & \ddots & \alpha_2^P \\ \alpha_2^P & \alpha_3^P & \cdots & \alpha_n^P & \alpha_1^P \end{pmatrix} \qquad M^P = \begin{pmatrix} \alpha_1^H & \alpha_2^H & \cdots & \alpha_{n-1}^H & \alpha_n^H \\ \alpha_n^H & \alpha_1^H & \alpha_2^H & & \alpha_{n-1}^H \\ \vdots & \alpha_n^H & \alpha_1^H & \ddots & \vdots \\ \alpha_3^H & & \ddots & \ddots & \alpha_2^H \\ \alpha_2^H & \alpha_3^H & \cdots & \alpha_n^H & \alpha_1^H \end{pmatrix} \tag{2.3}$$

2.2 Replicator dynamics

2.2.1 Single population dynamics

To introduce replicator dynamics we first consider one species with two types x and y. The change of frequency of the two types is then dependent on the fitness of the respective types f_x and f_y. As a normalisation, the average fitness $\overline{f} = xf_x + yf_y$ is subtracted.

$$\dot{x} = x\left(f_x - \overline{f}\right) \qquad \text{and} \qquad \dot{y} = y\left(f_y - \overline{f}\right) \tag{2.4}$$

The fitness is expressed through payoffs of interactions between the species. A general payoff matrix can then be written as

$$\begin{array}{cc} & \begin{array}{cc} x & y \end{array} \\ \begin{array}{c} x \\ y \end{array} & \begin{pmatrix} a & b \\ c & d \end{pmatrix}. \end{array} \tag{2.5}$$

For example c is the benefit of the second type with frequency y (row two) interacting with the first type with frequency x (column one). The fitness for the types is then

$$f_x = xa + yb \qquad \text{and} \qquad f_y = xc + yd. \tag{2.6}$$

The frequencies x and y are always between 0 and 1 because of the normalisation. The total population size stays constant $x+y=1$ and the total change of population size is zero $\dot{x}+\dot{y}=0$. The frequency of the second type can therefore be expressed as $y = 1 - x$. Taking this into account Equations 2.4 are reduced to one equation

$$\dot{x} = x\left(1 - x\right)\left(f_x - f_y\right). \tag{2.7}$$

This is termed replicator equation [Nowak, 2006; Zeeman, 1980; Taylor and Jonker, 1978] and used widely in evolutionary game dynamics.

2.2.2 Two population dynamics

Extending replicator dynamics to host and parasite systems comes with a two-species model which fundamentally changes the replicator dynamics. Host fitness is only influenced by interactions with parasites and parasite fitness is only influenced by hosts. The change in allele frequency of host (h) and parasite (p) types ($i = 1, ..., n$) depends on the respective host and parasite frequencies and the fitness of the types f_i minus an average fitness $\overline{f}$

$$\dot{h}_i = h_i\left(f_i^H - \overline{f}^H\right) \qquad \text{and} \qquad \dot{p}_i = p_i\left(f_i^P - \overline{f}^P\right). \tag{2.8}$$

Again, replicator dynamics are characterised by a constant population size normalised to one. But this time, because there are two species, the normalisation is within one species $\sum_{i=1}^{n} h_i = 1$ and $\sum_{i=1}^{n} p_i = 1$. From this it follows that the total change in frequency $\frac{d}{dt}h$ and $\frac{d}{dt}p$ of host and parasite is zero respectively: $\sum_{i=1}^{n} \dot{h}_i = 0$ and $\sum_{i=1}^{n} \dot{p}_i = 0$. This leads to the following set of differential equations

$$\dot{h}_i = h_i \left(f_i^H - \sum_{k=1}^{n} h_k f_k^H \right) \qquad \text{and} \qquad \dot{p}_i = p_i \left(f_i^P - \sum_{k=1}^{n} p_k f_k^P \right), \tag{2.9}$$

where f_i^H is a function of all parasite type frequencies p_k and f_i^P is a function of h_k, $k = 1, 2, ..., n$. A fundamental property of this system is the reducibility of the number of differential equations owing to the normalisation. The state space is now $2(n-1)$ −dimensional and can be formulated as two $(n-1)$ −simplices.
The fitness of hosts can now be expressed with the payoff matrices M^H and M^P, so that $f_i^H = \left(M^H p\right)_i$ and $f_i^P = \left(M^P h\right)_i$. Here $h = (h_1, h_2, ..., h_n)^T$ and $p = (p_1, p_2, ..., p_n)^T$ are the vectors with relative host and parasite frequencies of each type. The differential equations for replicator dynamics are therefore

$$\dot{h}_i = h_i \left(\left(M^H p\right)_i - h^T M^H p \right) \qquad \text{and} \qquad \dot{p}_i = p_i \left(\left(M^P h\right)_i - p^T M^P h \right). \tag{2.10}$$

The specific models, defined by the payoff matrices in Section 2.1 are now employed to replicator dynamics

Matching allele

Even though this model is based on interaction between matching types, it is important to realise that owing to the constant population size there is an indirect effect of other hosts and parasites on one another. Biologically this reflects competition between hosts. For example, if one host increases fast in numbers or when space, food or other resources are limited other hosts suffer from the increase of that specific type. Nevertheless, the average payoff is the same for each type so that trends can still be analysed but in a limited parameter space. Applying the matching allele fitness effects to replicator dynamics leads to the following set of differential equations which describe the frequency change of host and parasite types.

$$\dot{h}_i = h_i \left(-p_i + \sum_{k=1}^{n} h_k p_k \right) \qquad \dot{p}_i = p_i \left(h_i - \sum_{k=1}^{n} h_k p_k \right) \tag{2.11}$$

Cross-infection

It is possible to simplify the notation of the differential equations as follows because of the periodic boundary condition with $p_0 = p_n$, $p_{n+1} = p_1$, $h_0 = h_n$ and $h_{n+1} = h_1$.

$$\dot{h}_i = h_i \left(-\left(p_{i-1} + p_i + p_{i+1}\right) + \sum_{k=1}^{n} h_k \left(p_{k-1} + p_k + p_{k+1}\right) \right) \tag{2.12}$$

$$\dot{p}_i = p_i \left(\left(h_{i-1} + h_i + h_{i+1}\right) - \sum_{k=1}^{n} p_k \left(h_{k-1} + h_k + h_{k+1}\right) \right) \tag{2.13}$$

General infection

The differential equations are now more complicated, so that it is best to present the general form like in Equation 2.10.

$$\dot{h}_i = h_i \left(\left(M^H p\right)_i - h^T M^H p \right) \qquad \dot{p}_i = p_i \left(\left(M^P h\right)_i - p^T M^P h \right) \tag{2.14}$$

2.3 Lotka-Volterra dynamics

Lotka-Volterra dynamics are usually employed to describe predator-prey systems where the prey reproduces at a constant rate and the predator dies at a constant rate. The growth rate of the predator, however, is influenced by the abundance of prey and the prey numbers are diminished by the predators.

The same concept is applied to host-parasite systems with a constant birth-rate for the host b_h and a constant parasite death-rate d_p.

$$\dot{h}_i = h_i \left(f_i^H + b_h \right) \qquad \dot{p}_i = p_i \left(f_i^P - d_p \right) \tag{2.15}$$

There is no normalisation term to ensure a constant total population. We are now looking at abundances, not frequencies of the specific types. Like in the replicator dynamics model the fitness is defined by payoff matrices and the other species' abundances.

$$\dot{h}_i = h_i \left(\left(M^H p\right)_i + b_h \right) \qquad \dot{p}_i = p_i \left(\left(M^P h\right)_i - d_p \right) \tag{2.16}$$

Matching allele

As with the replicator dynamics we first focus on the simple matching allele model. Since b_h and d_p are constants the differential equations are decoupled from one another. We obtain n independent systems of two differential equations each.

$$\dot{h}_i = h_i \left(-p_i + b_h \right) \qquad \dot{p}_i = p_i \left(h_i - d_p \right) \tag{2.17}$$

This makes the Lotka-Volterra matching allele model a limiting case, with particularly simple dynamics.

Cross-infection

The differential equations are now connected to each other by types $i \pm 1$,

$$\dot{h}_i = h_i \left(-\left(p_{i-1} + p_i + p_{i+1}\right) + b_h \right) \qquad \dot{p}_i = p_i \left(\left(h_{i-1} + h_i + h_{i+1}\right) - d_p \right) \tag{2.18}$$

with $p_0 = p_n$, $p_{n+1} = p_1$, $h_0 = h_n$ and $h_{n+1} = h_1$.

General infection

Utilising the most general payoff matrices leads to these general differential equations (2.16)

$$\dot{h}_i = h_i \left(\left(M^H p\right)_i + b_h \right) \qquad \text{and} \qquad \dot{p}_i = p_i \left(\left(M^P h\right)_i - d_p \right), \tag{2.19}$$

where p and h are the vectors containing all population sizes h_i and p_i for $i = 1, 2, ..., n$.

2.4 Numerical integration

A numerical analysis is conducted in `python` [van Rossum, 1995], starting with various initial conditions (frequencies or abundances of hosts and parasites) and numerically iterating over several generations. The resulting trajectories were studied more closely for the system of three hosts and parasites.

It has to be noted that solving the differential equations for several n was done using diverse integrators. `Python`'s built-in functions `odeint` and `integrate` (from `scipy.integrate`) often lead to results outside the simplex for replicator dynamics. This is why a normalisation $h_n = 1 - \sum_{i=1}^{n-1}$ was utilised. For all trajectories and Poincaré sections the built in function was used. For the chaos analysis the precision was not sufficient. This is why a precision of 300 bits was chosen in the `bigfloat` package which is approximately $300 \cdot \log_{10} 2 \approx 90$ decimal digits. Since the built-in integrators could not handle `bigfloat` numbers a four-step Runge-Kutta method was implemented manually.
The four-step Runge-Kutta update shows fundamentally different results even when precision is as high as 1000. Removing the restriction of constant population size from the Runge-Kutta integrator does not generate different results - the values stay in the simplex.

2.5 Fixed points and stability

A fixed point per definition is a state which does not change once reached. This means that the time derivation at this point is zero: $\dot{h}_i = 0$ and $\dot{p}_i = 0$. There are many trivial fixed points where one host or parasite type is nonexistent (one type h_i or p_i has frequency 0 or abundance 0). However, the fixed point in the interior of the simplex defined by the host/parasite populations (h^*, p^*) is of biological interest since this means a coexistence of all types. It is further worth knowing whether this is an attracting, repelling or neutrally stable point. This is done by calculating the eigenvalues of the Jacobian at the inner fixed point. The real part of the eigenvalues of this matrix gives insight into the stability of the point. If all are negative the fixed point is attractive, if at least one is positive it is a saddle (and repulsive if all are positive) and if all are zero it is neutrally stable. These statements hold locally, which means close to the point of interest, since this is where the Jacobian is evaluated. In the case of replicator dynamics it is necessary to reduce the number of differential equations to $2(n-1)$ because of the normalisation $\sum_{i=1}^{n} h_i = \sum_{i=1}^{n} p_i = 1$. The matrix now has full rank and the number of eigenvalues is always $2(n-1)$. In general the Jacobian is

$$J = \begin{pmatrix} \frac{\partial \dot{h}_1}{\partial h_1} & \cdots & \frac{\partial \dot{h}_1}{\partial h_{n-1}} & \frac{\partial \dot{h}_1}{\partial p_1} & \cdots & \frac{\partial \dot{h}_1}{\partial p_{n-1}} \\ \vdots & & \vdots & \vdots & & \vdots \\ \frac{\partial \dot{h}_{n-1}}{\partial h_1} & \cdots & \frac{\partial \dot{h}_{n-1}}{\partial h_{n-1}} & \frac{\partial \dot{h}_{n-1}}{\partial p_1} & \cdots & \frac{\partial \dot{h}_{n-1}}{\partial p_{n-1}} \\ & & & & & \\ \frac{\partial \dot{p}_1}{\partial h_1} & \cdots & \frac{\partial \dot{p}_1}{\partial h_{n-1}} & \frac{\partial \dot{p}_1}{\partial p_1} & \cdots & \frac{\partial \dot{p}_1}{\partial p_{n-1}} \\ \vdots & & \vdots & \vdots & & \vdots \\ \frac{\partial \dot{p}_{n-1}}{\partial h_1} & \cdots & \frac{\partial \dot{p}_{n-1}}{\partial h_{n-1}} & \frac{\partial \dot{p}_{n-1}}{\partial p_1} & \cdots & \frac{\partial \dot{p}_{n-1}}{\partial p_{n-1}} \end{pmatrix} \in \mathbb{R}^{2(n-1)\times 2(n-1)} \tag{2.20}$$

for the replicator dynamics, and similar in the Lotka-Volterra case but in $\mathbb{R}^{2n\times 2n}$, where the number of eigenvalues is $2n$.
For deriving fixed points and stability for fixed n `mathematica` [Wolfram Research, 2014] was of help.

2.6 Constant of motion

A constant of motion is usually formulated as a Hamilton function in physics. It can often be viewed as an energy function. The energy in an isolated system stays constant in time. This concept is transferred to dynamical systems where the function is not explicitly time-dependent. In this case we formulate a function $H(h_i, p_i)$ which stays constant in time

$$\frac{dH}{dt} = \dot{H} = 0. \tag{2.21}$$

We will see in the results section that this can be visualised in a two-dimensional system (replicator dynamics with two types of hosts and parasites or Lotka-Volterra dynamics with one type).
Again, `mathematica` [Wolfram Research, 2014] was useful to study constants of motion for fixed n.

2.7 Analysis of chaotic dynamics

While working on the differential equations it became clear that not all initial conditions of the system lead to simple orbits. In the replicator dynamics it is enough to look at the 3×3 case with three hosts and three parasites which reduces to a four-dimensional system. For the Lotka-Volterra system the 2×2 case is four-dimensional if the differential equations are not decoupled. These cases were analysed more closely by looking at projections into three-dimensional space and Poincaré sections with certain restraints [Sato et al., 2002]. Sensitive dependence on initial conditions are examined by estimating the largest Lyapunov exponents [Kim and Choe, 2010].

Poincaré sections

Poincaré sections are $(n-1)-$dimensional planes in an $n-$dimensional system where the normal vector of the plane is not orthogonal to any trajectories passing through the plane. This way dimensions are reduced and the trajectories can be visualised more simply. Poincaré sections from Sato et al. [2002] were reproduced successfully in `python` and the same method was applied to the matching allele 3×3 replicator dynamics model. The constraint used here was

$$h_2 - h_1 + p_2 - p_1 = 0. \tag{2.22}$$

Another Poincaré section using the constant of motion as a constraint was generated

$$\log h_1 h_2 h_3 - \log p_1 p_2 p_3 = 0. \tag{2.23}$$

The planes were plotted in the h_1/p_2-plane. Note that usually only passages through the section from one direction are plotted. In Figure 4.2 intersections from both sides were plotted.

Lyapunov exponents

Lyapunov exponents measure the exponential divergence rate of two close initial conditions. In [Kim and Choe, 2010] a method for estimating the largest Lyapunov exponent (without knowing the attractor) is introduced. Two close initial conditions, which satisfy Equation 2.26, are chosen. Another fixed parameter Δ is chosen which specifies a second distance for Equation 2.27. Now the time point is of interest after which the trajectories of the initially close conditions have diverged as far as this second distance.

We start with two initial conditions indexed by a and b

$$x(0)^a = [h(0)^a, p(0)^a]^T = [0.5, 0.01k, 0.5 - 0.01k, 0.5, 0.25, 0.25]^T \tag{2.24}$$

$$x(0)^b = \left[h(0)^b, p(0)^b\right]^T = \left[0.5, 0.01k + 10^{-d}k, 0.5 - 0.01k - 10^{-d}k, 0.5, 0.25, 0.25\right]^T, \tag{2.25}$$

with a maximum distance for fixed D

$$\|x(0)^a - x(0)^b\| \leq \mathrm{e}^{-D}. \tag{2.26}$$

For fixed Δ the following time is of interest

$$V(\Delta) = \inf\{t : \|x(t)^a - x(t)^b\| \geq \mathrm{e}^{-D+\Delta}\}, \tag{2.27}$$

where $x = (h, p)$ is the vector containing host and parasite frequencies at time t starting in $x(0)$. This is the time it takes for an initial distance defined by D to increase to a minimal distance defined by Δ. The divergence time should grow as Δ gets larger. However, too large values of Δ are not possible since trajectories are bound to a certain state space. For replicator dynamics $\Delta \leq D + \log 2$ holds because the distance of two points in each $2-$simplex cannot be larger than one. Assuming linear growth of $V(\Delta)$ with Δ, which corresponds to exponential divergence of initial conditions, $\frac{\Delta}{V(\Delta)}$ should be a constant which is the divergence velocity and therefore the estimated Lyapunov exponent λ_{max}.

2.8 Stochastic simulations

A three-type matching allele model can be analysed stochastically in an individual based model. Starting with a certain number of each type the following transitions are possible

$$H_i + P_i \xrightarrow{r_i} P_i + P_i \qquad H_i \xrightarrow{b_h} H_i + H_i \qquad P_i \xrightarrow{d_p} \text{-} \tag{2.28}$$

The first reaction is the classical reaction between a host and its matching parasite, where the host dies out and the parasite replicates with a rate r_i. Hosts replicate with rate b_h in the second reaction and parasites die out with d_p. The simulations are carried out using a Gillespie stochastic simulation algorithm [Gillespie, 2007; Quigley et al., 2012; McKane and Newman, 2004]. The simulation was started with 1000 hosts and 1000 parasites. Reaction rates: $r_i = 0.01$, $b_h = 5$, $d_p = 2.5$. The code is described in the Appendix, Section 6.3.

3 Analytical results

In the course of analysing the systems it became clear that certain symmetry assumptions had to be made to find some general results for stability and constant of motion. A circulant matrix with a different value on each diagonal did not result in a simple case of stability or a constant of motion. $M^H = -c \cdot \left(M^P\right)^T$ was therefore assumed.

3.1 Fixed points and stability

Solving the differential equations $\dot{h}_i\left(h^*, p^*\right) = 0$ and $\dot{p}_i\left(h^*, p^*\right) = 0$ leads to some trivial fixed points where at least one host or one parasite are non-existent. But the most interesting is the inner fixed point. For all replicator dynamics models (see Section 2.2.2) the inner fixed point is simply

$$h_i^* = p_i^* = \frac{1}{n}. \tag{3.1}$$

The three Lotka-Volterra models (Section 2.3) each have different inner fixed points depending on the number of interactions. For the Lotka-Volterra matching allele model the inner fixed point is

$$h_i^* = d_p \qquad \text{and} \qquad p_i^* = b_h. \tag{3.2}$$

For the Lotka-Volterra cross-infection model the inner fixed point is found to be

$$h_i^* = \frac{d_p}{3} \qquad \text{and} \qquad p_i^* = \frac{b_h}{3}. \tag{3.3}$$

For the most general Lotka-Volterra model the fixed point is

$$h_i^* = \frac{d_p}{\sum_{i=1}^{n} \alpha_i^H} \qquad \text{and} \qquad p_i^* = -\frac{b_h}{\sum_{i=1}^{n} \alpha_i^P}. \tag{3.4}$$

3.1.1 Replicator dynamics

Matching allele model

After reducing dimensions with $h_n = 1 - \sum_{i=1}^{n-1} h_i$ and $p_n = 1 - \sum_{i=1}^{n-1} p_i$ the differential equations are defined for $n = 1, 2, ..., n-1$:

$$\dot{h}_i = h_i \left(-p_i + \sum_{k=1}^{n-1} h_k p_k + \left(1 - \sum_{k=1}^{n-1} h_k\right)\left(1 - \sum_{k=1}^{n-1} p_k\right)\right) \tag{3.5}$$

and

$$\dot{p}_i = p_i \left(h_i - \sum_{k=1}^{n-1} h_k p_k - \left(1 - \sum_{k=1}^{n-1} h_k\right)\left(1 - \sum_{k=1}^{n-1} p_k\right)\right) \tag{3.6}$$

The exact form of the entries (partial derivatives in the general Jacobian matrix) are shown in the Appendix in 6.1
The Jacobian at the inner fixed point $h_i^* = p_i^* = \frac{1}{n}$ simplifies to

$$J\left(h^*, p^*\right) = \begin{pmatrix} & & -\frac{1}{n} & & 0 \\ & 0 & & \ddots & \\ & & 0 & & -\frac{1}{n} \\ \frac{1}{n} & 0 & & & \\ & \ddots & & 0 & \\ 0 & \frac{1}{n} & & & \end{pmatrix} \in \mathbb{R}^{2(n-1)\times 2(n-1)}. \tag{3.7}$$

The eigenvalues of the Jacobian are calculated via the determinant $det\left(J\left(h^*, p^*\right) - \lambda I_{2(n-1)}\right)$ which is not changed by adding multiples $\left(\frac{1}{\lambda n}\right)$ of the upper $n-1$ rows to the lower $n-1$. This leads to the following matrix

$$\begin{pmatrix} -\lambda & & & -\frac{1}{n} & & 0 \\ & \ddots & & & \ddots & \\ & & -\lambda & & & -\frac{1}{n} \\ & & & -\lambda - \frac{1}{\lambda n^2} & & \\ & 0 & & & \ddots & \\ & & & & & -\lambda - \frac{1}{\lambda n^2} \end{pmatrix}. \tag{3.8}$$

The determinant of any triangular matrix is just the product of the diagonal elements. This can be seen by doing a Laplace extension on the first column (and the first column of each submatrix). The following equation determines the eigenvalues:

$$\begin{aligned} 0 &= (-\lambda)^{n-1}\left(-\lambda - \frac{1}{\lambda n^2}\right)^{n-1} \\ &= \left(\lambda + i\frac{1}{n}\right)^{n-1}\left(\lambda - i\frac{1}{n}\right)^{n-1} \end{aligned} \tag{3.9}$$

It is easy to see that the eigenvalues are $\lambda = \pm i\frac{1}{n}$ with multiplicity $n-1$. This means that the inner fixed point is neutrally stable and the oscillation frequency close to this point is $\frac{1}{2\pi n}$. This implies that the period of the oscillation $2\pi n$ depends on the number of types of host and parasite. The more types the more complex the deterministic dynamics. To reach the initial conditions close to the fixed point in a system with n types takes n times longer than in a system with only one host and parasite type. In the case of replicator dynamics this is only logical, since the differential equations are not independent of one another but coupled through the average fitness $\overline{f}$ (normalisation term).

Cross-infection

All replicator dynamics equations can be reduced owing to the normalisation. Here we differentiate between type one, type n and all other types so that no new introduction of variables (e.g. $h_{n+1} = h_1$) is needed. The differential equations are

$$\dot{h}_1 = h_1 \left(- \left(1 - \sum_{k=3}^{n-1} p_k \right) - \overline{f}^H \right) \tag{3.10}$$

$$\dot{h}_i = h_i \left(- \left(p_i + p_i + p_{i+1} \right) - \overline{f}^H \right) \qquad \text{for} \quad i = 2, 3, ..., n-2 \tag{3.11}$$

$$\dot{h}_{n-1} = h_{n-1} \left(- \left(1 - \sum_{k=1}^{n-3} p_k \right) - \overline{f}^H \right), \tag{3.12}$$

with an average fitness for hosts

$$\begin{aligned} \overline{f}^H =& - h_1 \left(1 - \sum_{k=3}^{n-1} p_k \right) - \sum_{k=2}^{n-2} h_k \left(p_{k-1} + p_k + p_{k+1} \right) - h_{n-1} \left(1 - \sum_{k=1}^{n-3} p_k \right) \\ & - \left(1 - \sum_{k=1}^{n-1} h_k \right) \left(1 - \sum_{k=2}^{n-2} p_k \right), \end{aligned} \tag{3.13}$$

and similarly for the parasites

$$\dot{p}_1 = p_1 \left(\left(1 - \sum_{k=3}^{n-1} h_k \right) - \overline{f}^P \right) \tag{3.14}$$

$$\dot{p}_i = p_i \left(h_i + h_i + h_{i+1} - \overline{f}^P \right) \qquad \text{for} \quad i = 2, 3, ..., n-2 \tag{3.15}$$

$$\dot{p}_{n-1} = p_{n-1} \left(\left(1 - \sum_{k=1}^{n-3} h_k \right) - \overline{f}^P \right), \tag{3.16}$$

with an average parasite fitness

$$\begin{aligned} \overline{f}^P =& p_1 \left(1 - \sum_{k=3}^{n-1} h_k \right) + \sum_{k=2}^{n-2} p_k \left(h_{k-1} + h_k + h_{k+1} \right) + p_{n-1} \left(1 - \sum_{k=1}^{n-3} h_k \right) \\ & + \left(1 - \sum_{k=1}^{n-1} p_k \right) \left(1 - \sum_{k=2}^{n-2} h_k \right). \end{aligned} \tag{3.17}$$

The explicit terms for the Jacobian can be found in the Appendix 6.1. Inserting the inner fixed point results in the following Jacobian matrix

$$J\left(h^*, p^*\right) = \begin{pmatrix} 0 & A \\ -A & 0 \end{pmatrix} \in \mathbb{R}^{2(n-1) \times 2(n-1)}, \tag{3.18}$$

with

$$A = \begin{pmatrix} 0 & 0 & \frac{1}{n} & \frac{1}{n} & \cdots & \frac{1}{n} \\ -\frac{1}{n} & -\frac{1}{n} & -\frac{1}{n} & 0 & \cdots & 0 \\ 0 & -\frac{1}{n} & -\frac{1}{n} & -\frac{1}{n} & \ddots & \vdots \\ \vdots & \ddots & \ddots & \ddots & \ddots & 0 \\ 0 & \cdots & 0 & -\frac{1}{n} & -\frac{1}{n} & -\frac{1}{n} \\ \frac{1}{n} & \cdots & \frac{1}{n} & \frac{1}{n} & 0 & 0 \end{pmatrix} \in \mathbb{R}^{(n-1) \times (n-1)}. \tag{3.19}$$

The stability of the inner fixed point is determined via the eigenvalues of the Jacobian.

$$0 = det\left(J\left(h^*, p^*\right) - \lambda I_{2(n-1)}\right) = det\begin{pmatrix} -\lambda I_{n-1} & A \\ A & -\lambda I_{n-1} \end{pmatrix} \tag{3.20}$$

Using linear combinations of the first $n-1$ rows added to the last $n-1$ rows one gets:

$$0 = det\begin{pmatrix} -\lambda I_{n-1} & A \\ 0 & B \end{pmatrix} = det\left(-\lambda I_{n-1}\right) det\left(B\right) = \left(-\lambda\right)^{n-1} det\left(B\right), \tag{3.21}$$

this equation follows immediately from the Laplace expansion.

$$B = \begin{pmatrix}
-\lambda+\frac{1}{n^2\lambda} & 0 & -\frac{1}{n^2\lambda} & -\frac{2}{n^2\lambda} & \cdots & \cdots & \cdots & -\frac{2}{n^2\lambda} & -\frac{1}{n^2\lambda} \\
\frac{1}{n^2\lambda} & -\lambda+\frac{2}{n^2\lambda} & \frac{1}{n^2\lambda} & 0 & -\frac{1}{n^2\lambda} & \cdots & \cdots & \cdots & -\frac{1}{n^2\lambda} \\
\frac{1}{n^2\lambda} & \frac{2}{n^2\lambda} & -\lambda+\frac{3}{n^2\lambda} & \frac{2}{n^2\lambda} & \frac{1}{n^2\lambda} & 0 & \cdots & \cdots & 0 \\
0 & \frac{1}{n^2\lambda} & \frac{2}{n^2\lambda} & -\lambda+\frac{3}{n^2\lambda} & \frac{2}{n^2\lambda} & \frac{1}{n^2\lambda} & 0 & \cdots & 0 \\
\vdots & \vdots & \vdots & \vdots & \vdots & \vdots & \vdots & \vdots & \vdots \\
0 & \cdots & \cdots & 0 & \frac{1}{n^2\lambda} & \frac{2}{n^2\lambda} & -\lambda+\frac{3}{n^2\lambda} & \frac{2}{n^2\lambda} & \frac{1}{n^2\lambda} \\
-\frac{1}{n^2\lambda} & \cdots & \cdots & \cdots & -\frac{1}{n^2\lambda} & 0 & \frac{1}{n^2\lambda} & -\lambda+\frac{2}{n^2\lambda} & \frac{1}{n^2\lambda} \\
-\frac{1}{n^2\lambda} & -\frac{2}{n^2\lambda} & \cdots & \cdots & \cdots & -\frac{2}{n^2\lambda} & -\frac{1}{n^2\lambda} & 0 & -\lambda+\frac{1}{n^2\lambda}
\end{pmatrix} \tag{3.22}$$

B is still not a triangular matrix, the determinant is not solved easily for general n. The stability analysis is therefore described for several fixed n.

For $n = 4$ we get

$$B = \begin{pmatrix} -\lambda - \frac{1}{16\lambda} & 0 & 0 \\ 0 & -\lambda - \frac{1}{16\lambda} & 0 \\ 0 & 0 & -\lambda - \frac{1}{16\lambda} \end{pmatrix}. \tag{3.23}$$

The eigenvalues are therefore calculated as follows:

$$0 = \left(-\lambda\right)^3 \left(-\lambda - \frac{1}{16\lambda}\right)^3, \tag{3.24}$$

which gives

$$\lambda = \pm\frac{i}{4} \qquad \text{with multiplicity 3.} \tag{3.25}$$

The inner fixed point for $n = 4$ is neutrally stable.

For $n = 5$ we get

$$B = \begin{pmatrix} -\lambda - \frac{1}{25\lambda} & 0 & \frac{1}{25\lambda} & \frac{1}{25\lambda} \\ -\frac{1}{25\lambda} & -\lambda - \frac{2}{25\lambda} & -\frac{1}{25\lambda} & 0 \\ 0 & -\frac{1}{25\lambda} & -\lambda - \frac{2}{25\lambda} & -\frac{1}{25\lambda} \\ \frac{1}{25\lambda} & \frac{1}{25\lambda} & 0 & -\lambda - \frac{1}{25\lambda} \end{pmatrix}. \tag{3.26}$$

Trigonalising this matrix gives

$$C = \begin{pmatrix} -\lambda - \frac{1}{25\lambda} & 0 & \frac{1}{25\lambda} & \frac{1}{25\lambda} \\ 0 & -\lambda - \frac{2}{25\lambda} & -\frac{2+25\lambda^2}{25(\lambda+25\lambda^3)} & -\frac{1}{25(\lambda+25\lambda^3)} \\ 0 & 0 & -\frac{1+75\lambda^2+625\lambda^4}{25(\lambda+25\lambda^3)} & -\frac{1+75\lambda^2+625\lambda^4}{25(2\lambda+75\lambda^3+625\lambda^5)} \\ 0 & 0 & 0 & -\frac{1+75\lambda^2+625\lambda^4}{25(2\lambda+25\lambda^3)} \end{pmatrix}. \tag{3.27}$$

The eigenvalues are therefore calculated as follows:

$$\begin{aligned} 0 &= (-\lambda)^4 \, det\,(B) = \left(-\lambda^4\right) det\,(C) \\ &= (-\lambda)^4 \left(-\lambda - \frac{1}{25\lambda}\right)\left(-\lambda - \frac{2}{25\lambda}\right)\left(-\frac{1+75\lambda^2+625\lambda^4}{25\left(\lambda+25\lambda^3\right)}\right)\left(-\frac{1+75\lambda^2+625\lambda^4}{25\left(2\lambda+25\lambda^3\right)}\right) \\ &= \frac{1}{25^4}\left(1+75\lambda^2+625\lambda^4\right)^2, \end{aligned} \tag{3.28}$$

so the following polynomial has to be solved. For this we define $l := \lambda^2$

$$0 = l^2 + \frac{75}{625} l + \frac{1}{625}, \tag{3.29}$$

which gives

$$l = -\frac{3 \pm \sqrt{5}}{50}, \tag{3.30}$$

and therefore the eigenvalues

$$\begin{aligned} \lambda &= \pm\sqrt{l} \\ &= \pm\frac{i}{5}\sqrt{\frac{1}{2}\left(3 \pm \sqrt{5}\right)} \qquad \text{each with multiplicity 2.} \end{aligned} \tag{3.31}$$

The inner fixed point for $n = 5$ is neutrally stable.

For $n = 6$ we get

$$B = \begin{pmatrix} -\lambda - \frac{1}{36\lambda} & 0 & \frac{1}{36\lambda} & \frac{1}{18\lambda} & \frac{1}{36\lambda} \\ -\frac{1}{36\lambda} & -\lambda - \frac{1}{18\lambda} & -\frac{1}{36\lambda} & 0 & \frac{1}{36\lambda} \\ -\frac{1}{36\lambda} & -\frac{1}{18\lambda} & -\lambda - \frac{1}{12\lambda} & -\frac{1}{18\lambda} & -\frac{1}{36\lambda} \\ \frac{1}{36\lambda} & 0 & -\frac{1}{36\lambda} & -\lambda - \frac{1}{18\lambda} & -\frac{1}{36\lambda} \\ \frac{1}{36\lambda} & \frac{1}{18\lambda} & \frac{1}{36\lambda} & 0 & -\lambda - \frac{1}{36\lambda} \end{pmatrix}. \tag{3.32}$$

Trigonalising this matrix gives

$$C = \begin{pmatrix} -\lambda - \frac{1}{36\lambda} & 0 & \frac{1}{36\lambda} & \frac{1}{18\lambda} & \frac{1}{36\lambda} \\ 0 & -\lambda - \frac{1}{18\lambda} & -\frac{1+18\lambda^2}{18(\lambda+36\lambda^3)} & -\frac{1}{18(\lambda+36\lambda^3)} & \frac{\lambda}{1+36\lambda^2} \\ 0 & 0 & -\frac{1+72\lambda^2+648\lambda^4}{18(\lambda+36\lambda^3)} & -\frac{1+72\lambda^2+648\lambda^4}{18(\lambda+54\lambda^3+648\lambda^5)} & -\frac{1+54\lambda^2+324\lambda^4}{18(\lambda+54\lambda^3+648\lambda^5)} \\ 0 & 0 & 0 & -\frac{2\lambda+18\lambda^3}{1+18\lambda^2} & -\frac{36\lambda^3+936\lambda^5}{(1+18\lambda^2)(1+72\lambda^2+648\lambda^4)} \\ 0 & 0 & 0 & 0 & -\frac{2\lambda\left(1+9\lambda^2\right)\left(1+36\lambda^2\right)}{1+72\lambda^2+648\lambda^4} \end{pmatrix}. \tag{3.33}$$

The eigenvalues are therefore calculated as follows:

$$\begin{aligned}0 =& (-\lambda)^5 \, det\,(B) = \left(-\lambda^5\right) det\,(C) \\ =& (-\lambda)^5 \left(-\lambda - \frac{1}{36\lambda}\right) \left(-\lambda - \frac{1}{18\lambda}\right) \left(-\frac{1 + 72\lambda^2 + 648\lambda^4}{18\left(\lambda + 36\lambda^3\right)}\right) \\ & \left(-\frac{2\lambda + 18\lambda^3}{1 + 18\lambda^2}\right) \left(-\frac{2\lambda\left(1 + 9\lambda^2\right)\left(1 + 36\lambda^2\right)}{1 + 72\lambda^2 + 648\lambda^4}\right) \\ =& \frac{4\lambda^4}{9 \cdot 36^2}\left(1 + 9\lambda^2\right)^2 \left(1 + 36\lambda^2\right),\end{aligned} \tag{3.34}$$

the solutions of this polynomial are

$$\begin{aligned}\lambda_1 &= 0 && \text{with multiplicity 4,} \\ \lambda_2 &= \pm\frac{i}{3} && \text{each with multiplicity 2,} \\ \lambda_3 &= \pm\frac{i}{6} && \text{with multiplicity 1.}\end{aligned} \tag{3.35}$$

The inner fixed point for $n = 6$ is neutrally stable.

It was not possible to determine the stability of the inner fixed point for general n analytically. However, in cases where n was a fixed number $(3, 4, ..., 7)$ the result was neutral stability.

General infection

For the most general model we assume that

$$M^H = -c \cdot \left(M^P\right)^T . \tag{3.36}$$

Biologically this makes sense: a specific parasite type (for example parasite 4) has a negative influence on a specific host (type 2). The payoff for the host is the negative entry $\left(M^H\right)_{2,4}$. The parasite is influenced in the same, but positive (and possibly scaled) way $\left(M^P\right)_{4,2} = -c \cdot \left(M^H\right)_{2,4}$.

Because of the high number of parameters we will only discuss the case with $n = 3$ hosts and parasites. Here $\alpha_1^P = -c\alpha_1^H$, $\alpha_2^P = -c\alpha_3^H$ and $\alpha_3^P = -c\alpha_2^H$. Due to the normalisation (constant population size)

$$\dot{h_1} = h_1 \left(\alpha_1^P p_1 + \alpha_2^P p_2 + \alpha_3^P \left(1 - p_1 - p_2\right) - \overline{f}^H\right) \tag{3.37}$$

$$\dot{h_2} = h_2 \left(\alpha_3^P p_1 + \alpha_1^P p_2 + \alpha_2^P \left(1 - p_1 - p_2\right) - \overline{f}^H\right) \tag{3.38}$$

$$\dot{p_1} = p_1 \left(\alpha_1^H h_1 + \alpha_2^H h_2 + \alpha_3^H \left(1 - h_1 - h_2\right) - \overline{f}^P\right) \tag{3.39}$$

$$\dot{p_2} = p_2 \left(\alpha_3^H h_1 + \alpha_1^H h_2 + \alpha_2^H \left(1 - h_1 - h_2\right) - \overline{f}^P\right), \tag{3.40}$$

with an average fitness

$$\begin{aligned}\overline{f}^{H} &= h_1\left(\alpha_1^P p_1 + \alpha_2^P p_2 + \alpha_3^P\left(1-p_1-p_2\right)\right) + h_2\left(\alpha_3^P p_1 + \alpha_1^P p_2 + \alpha_2^P\left(1-p_1-p_2\right)\right)\\ &\quad + \left(1-h_1-h_2\right)\left(\alpha_2^P p_1 + \alpha_3^P p_2 + \alpha_1^P\left(1-p_1-p_2\right)\right) \qquad (3.41)\\ \overline{f}^{P} &= p_1\left(\alpha_1^H h_1 + \alpha_2^H h_2 + \alpha_3^H\left(1-h_1-h_2\right)\right) + p_2\left(\alpha_3^H h_1 + \alpha_1^H h_2 + \alpha_2^H\left(1-h_1-h_2\right)\right)\\ &\quad + \left(1-p_1-p_2\right)\left(\alpha_2^H h_1 + \alpha_3^H h_2 + \alpha_1^H\left(1-h_1-h_2\right)\right). \qquad (3.42)\end{aligned}$$

If we define $\Gamma_{i,j} = \alpha_i^H - \alpha_j^H$ for $i < j$ the Jacobian is

$$\begin{aligned} J\left(h^*, p^*\right) &= \begin{pmatrix} 0 & 0 & \frac{1}{3}\left(\alpha_1^P - \alpha_3^P\right) & \frac{1}{3}\left(\alpha_2^P - \alpha_3^P\right)\\ 0 & 0 & \frac{1}{3}\left(\alpha_3^P - \alpha_2^P\right) & \frac{1}{3}\left(\alpha_1^P - \alpha_2^P\right)\\ \frac{1}{3}\Gamma_{1,3} & \frac{1}{3}\Gamma_{2,3} & 0 & 0\\ -\frac{1}{3}\Gamma_{2,3} & \frac{1}{3}\Gamma_{1,2} & 0 & 0 \end{pmatrix} \qquad (3.43)\\ &= \begin{pmatrix} 0 & 0 & -\frac{c}{3}\Gamma_{1,2} & \frac{c}{3}\Gamma_{2,3}\\ 0 & 0 & \frac{c}{3}\Gamma_{2,3} & -\frac{c}{3}\Gamma_{1,3}\\ \frac{1}{3}\Gamma_{1,3} & \frac{1}{3}\Gamma_{2,3} & 0 & 0\\ -\frac{1}{3}\Gamma_{2,3} & \frac{1}{3}\Gamma_{1,2} & 0 & 0 \end{pmatrix}. \end{aligned}$$

Eigenvalues are calculated by

$$0 = det\left(J\left(h*, p*\right) - \lambda I_4\right) = det\left(B\right). \qquad (3.44)$$

Trigonalisation yields

$$B = \begin{pmatrix} -\lambda & 0 & -\frac{c}{3}\Gamma_{1,2} & \frac{c}{3}\Gamma_{2,3}\\ 0 & -\lambda & -\frac{c}{3}\Gamma_{2,3} & \frac{c}{3}\Gamma_{1,3}\\ 0 & 0 & -\lambda + \frac{c}{9\lambda}\left(\Gamma_{2,3}^2 - \Gamma_{1,2}\Gamma_{1,3}\right) & 0\\ 0 & 0 & 0 & -\lambda + \frac{c}{9\lambda}\left(-\Gamma_{1,3}\Gamma_{1,2} - \Gamma_{2,3}^2\right) \end{pmatrix}. \qquad (3.45)$$

In this very general case the four eigenvalues depend on the payoffs:

$$\lambda = \pm\frac{\sqrt{c}}{3}\sqrt{\pm\left(\alpha_2^H - \alpha_3^H\right) - \left(\alpha_1^H - \alpha_2^H\right)\left(\alpha_1^H - \alpha_3^H\right)} \qquad (3.46)$$

The inner fixed point is neutrally stable if the term under the square root is negative in all cases. If we assume that for matching hosts and parasites the payoff is maximal then α_1^H is the largest payoff. Assuming that neighbouring hosts are less suitable for the parasite $\alpha_1^H \gg \alpha_2^H > \alpha_3^H$ the fixed point is neutrally stable. The eigenvalues are imaginary and therefore the real part zero. If however there are two significant host types for each parasite and only one host is unsuitable $\alpha_1^H > \alpha_2^H \gg \alpha_3^H$ then for two eigenvalues we have $\lambda = \pm\frac{\sqrt{c}}{3}\sqrt{\left(\alpha_2^H - \alpha_3^H\right) - \left(\alpha_1^H - \alpha_2^H\right)\left(\alpha_1^H - \alpha_3^H\right)}$. Now since $\alpha_2^H - \alpha_3^H$ is very large the term under the square root is positive, the two eigenvalues are therefore real and one of them is positive. We now have a saddle. In other cases it depends on the value of the real part of the eigenvalues. When all eigenvalues are positive the fixed point is not stable (repulsive) if all are negative then the fixed point is stable (attractive).

3.1.2 Lotka-Volterra

Matching allele model

The Jacobian for the differential equations is

$$J = \begin{pmatrix} b_h - p_1 & & 0 & -h_1 & & 0 \\ & \ddots & & & \ddots & \\ 0 & & b_h - p_n & 0 & & -h_n \\ p_1 & & 0 & h_1 - d_p & & 0 \\ & \ddots & & & \ddots & \\ 0 & & p_n & 0 & & h_n - d_p \end{pmatrix} \in \mathbb{R}^{2n\times 2n}.$$

At the inner fixed point this simplifies to the following matrix

$$J\left(h^*, p^*\right) = \begin{pmatrix} & & & -d_p & & 0 \\ & \Large 0 & & & \ddots & \\ & & & 0 & & -d_p \\ b_h & & 0 & & & \\ & \ddots & & & \Large 0 & \\ 0 & & b_h & & & \end{pmatrix}. \tag{3.47}$$

Like in the replicator dynamics matching allele model the eigenvalues can be determined by adding multiples $\left(\frac{b_h}{\lambda}\right)$ of the first rows to the last rows of $J\left(h^*, p^*\right) - \lambda I_{2n}$ and setting the determinant zero. This leads to the following equation

$$\begin{aligned} 0 &= (-\lambda)^n \left(-\lambda - \frac{b_h}{\lambda}\right) \qquad (3.48) \\ &= \left(\lambda^2 + d_p b_h\right)^n \\ &= \left((\lambda)^2 - \left(i\sqrt{d_p b_h}\right)^2\right)^n \\ &= \left(\lambda + i\sqrt{d_p b_h}\right)^n \left(\lambda - i\sqrt{d_p b_h}\right)^n . \end{aligned}$$

It is easy to see that the eigenvalues are $\lambda = \pm i\sqrt{d_p b_h}$ with multiplicity n. Note that the eigenvalues do not depend on n and the differential equations for this model are independent for each type. The real part is zero, this means that the inner fixed point is neutrally stable and the oscillation frequency is

$$\frac{\sqrt{d_p b_h}}{2\pi}. \tag{3.49}$$

The period of the oscillations close to the fixed point in the matching allele model using replicator dynamics or Lotka-Volterra dynamics is therefore $\frac{2\pi}{\sqrt{h_i^* p_i^*}}$.

Cross-infection

Like in the replicator dynamics case the Jacobian can be written as

$$J\left(h^*, p^*\right) = \begin{pmatrix} 0 & A \\ B & 0 \end{pmatrix} \in \mathbb{R}^{2n\times 2n}, \tag{3.50}$$

with

$$A = \begin{pmatrix} -\frac{d_p}{3} & -\frac{d_p}{3} & 0 & 0 & \cdots & -\frac{d_p}{3} \\ -\frac{d_p}{3} & -\frac{d_p}{3} & -\frac{d_p}{3} & 0 & \cdots & 0 \\ 0 & -\frac{d_p}{3} & -\frac{d_p}{3} & -\frac{d_p}{3} & \cdots & 0 \\ \vdots & \vdots & \ddots & \ddots & \ddots & \vdots \\ 0 & 0 & \cdots & -\frac{d_p}{3} & -\frac{d_p}{3} & -\frac{d_p}{3} \\ -\frac{d_p}{3} & 0 & \cdots & 0 & -\frac{d_p}{3} & -\frac{d_p}{3} \end{pmatrix}, \qquad B = \begin{pmatrix} \frac{b_h}{3} & \frac{b_h}{3} & 0 & 0 & \cdots & \frac{b_h}{3} \\ \frac{b_h}{3} & \frac{b_h}{3} & \frac{b_h}{3} & 0 & \cdots & 0 \\ 0 & \frac{b_h}{3} & \frac{b_h}{3} & \frac{b_h}{3} & \cdots & 0 \\ \vdots & \vdots & \ddots & \ddots & \ddots & \vdots \\ 0 & 0 & \cdots & \frac{b_h}{3} & \frac{b_h}{3} & \frac{b_h}{3} \\ \frac{b_h}{3} & 0 & \cdots & 0 & \frac{b_h}{3} & \frac{b_h}{3} \end{pmatrix}. \tag{3.51}$$

For specific n the eigenvalues are calculated.

When $n = 4$ and trigonalising the matrix the polynomial already becomes more complicated

$$det(J - \lambda I_8) = det \begin{pmatrix} -\lambda & 0 & 0 & 0 & -\frac{d_p}{3} & -\frac{d_p}{3} & 0 & -\frac{d_p}{3} \\ 0 & -\lambda & 0 & 0 & -\frac{d_p}{3} & -\frac{d_p}{3} & -\frac{d_p}{3} & 0 \\ 0 & 0 & -\lambda & 0 & 0 & -\frac{d_p}{3} & -\frac{d_p}{3} & -\frac{d_p}{3} \\ 0 & 0 & 0 & -\lambda & -\frac{d_p}{3} & 0 & -\frac{d_p}{3} & -\frac{d_p}{3} \\ 0 & 0 & 0 & 0 & & & & \\ 0 & 0 & 0 & 0 & & & & \\ 0 & 0 & 0 & 0 & & C & & \\ 0 & 0 & 0 & 0 & & & & \end{pmatrix}, \tag{3.52}$$

with

$$C = \begin{pmatrix} -\lambda - \frac{b_h d_p}{3\lambda} & -\frac{2b_h d_p}{9\lambda} & -\frac{2b_h d_p}{9\lambda} & -\frac{2b_h d_p}{9\lambda} \\ 0 & -\lambda - \frac{b_h d_p\left(5b_h d_p+27\lambda^2\right)}{27b_h d_p\lambda+81\lambda^3} & -\frac{b_h d_p\left(2b_h d_p+18\lambda^2\right)}{27b_h d_p\lambda+81\lambda^3} & -\frac{b_h d_p\left(2b_h d_p+18\lambda^2\right)}{27b_h d_p\lambda+81\lambda^3} \\ 0 & 0 & -\lambda - \frac{b_h d_p\left(7b_h d_p+27\lambda^2\right)}{45b_h d_p\lambda+81\lambda^3} & -\frac{b_h d_p\left(2b_h d_p+18\lambda^2\right)}{45b_h d_p\lambda+81\lambda^3} \\ 0 & 0 & 0 & -\lambda - \frac{b_h d_p\left(b_h d_p+3\lambda^3\right)}{7b_h d_p\lambda+9\lambda^3} \end{pmatrix}. \tag{3.53}$$

The product of the diagonal entries is the determinant, which, set to zero, generates the eigenvalues

$$\lambda_1 = \pm\frac{i}{3}\sqrt{b_h d_p} \qquad \text{each with multiplicity 3,} \tag{3.54}$$

$$\lambda_2 = \pm i\sqrt{b_h d_p} \qquad \text{each with multiplicity 1.}$$

The inner fixed point for $n = 4$ is neutrally stable.

For $n = 5$ the eigenvalues are

$$\lambda_1 = \pm\frac{i}{3\sqrt{2}}\sqrt{\left(3 \pm \sqrt{5}\right) b_h d_p} \qquad \text{each with multiplicity 2,} \tag{3.55}$$

$$\lambda_2 = \pm i\sqrt{b_h d_p} \qquad \text{each with multiplicity 1.}$$

The inner fixed point for $n = 5$ is neutrally stable.

For $n = 6$ the eigenvalues are

$$\begin{aligned}
\lambda_1 &= 0 \qquad \text{with multiplicity 4,} \\
\lambda_2 &= \pm\frac{i}{3}\sqrt{b_h d_p} \qquad \text{each with multiplicity 1,} \\
\lambda_3 &= \pm\frac{2i}{3}\sqrt{b_h d_p} \qquad \text{each with multiplicity 2,} \\
\lambda_4 &= \pm i\sqrt{b_h d_p} \qquad \text{each with multiplicity 1.}
\end{aligned} \tag{3.56}$$

The inner fixed point for $n = 6$ is neutrally stable.

In all cases analysed the inner fixed point showed neutral stability.

General infection

Similarly to the above model the most general case becomes very complicated for n types. Even the model with 3 types proves difficult. The Jacobian can be written as

$$J\left(h^*, p^*\right) = \begin{pmatrix} 0 & A \\ B & 0 \end{pmatrix} \in \mathbb{R}^{2n\times 2n}, \tag{3.57}$$

with

$$A = \begin{pmatrix}
-\frac{cd_p\alpha_1^H}{\alpha_1^H+\alpha_2^H+\alpha_3^H} & -\frac{cd_p\alpha_3^H}{\alpha_1^H+\alpha_2^H+\alpha_3^H} & -\frac{cd_p\alpha_2^H}{\alpha_1^H+\alpha_2^H+\alpha_3^H} \\
-\frac{cd_p\alpha_2^H}{\alpha_1^H+\alpha_2^H+\alpha_3^H} & -\frac{cd_p\alpha_1^H}{\alpha_1^H+\alpha_2^H+\alpha_3^H} & -\frac{cd_p\alpha_3^H}{\alpha_1^H+\alpha_2^H+\alpha_3^H} \\
-\frac{cd_p\alpha_3^H}{\alpha_1^H+\alpha_2^H+\alpha_3^H} & -\frac{cd_p\alpha_2^H}{\alpha_1^H+\alpha_2^H+\alpha_3^H} & -\frac{cd_p\alpha_1^H}{\alpha_1^H+\alpha_2^H+\alpha_3^H}
\end{pmatrix} \tag{3.58}$$

and

$$B = \begin{pmatrix}
\frac{b_h\alpha_1^H}{c\left(\alpha_1^H+\alpha_2^H+\alpha_3^H\right)} & \frac{b_h\alpha_2^H}{c\left(\alpha_1^H+\alpha_2^H+\alpha_3^H\right)} & \frac{b_h\alpha_3^H}{c\left(\alpha_1^H+\alpha_2^H+\alpha_3^H\right)} \\
\frac{b_h\alpha_3^H}{c\left(\alpha_1^H+\alpha_2^H+\alpha_3^H\right)} & \frac{b_h\alpha_1^H}{c\left(\alpha_1^H+\alpha_2^H+\alpha_3^H\right)} & \frac{b_h\alpha_2^H}{c\left(\alpha_1^H+\alpha_2^H+\alpha_3^H\right)} \\
\frac{b_h\alpha_2^H}{c\left(\alpha_1^H+\alpha_2^H+\alpha_3^H\right)} & \frac{b_h\alpha_3^H}{c\left(\alpha_1^H+\alpha_2^H+\alpha_3^H\right)} & \frac{b_h\alpha_1^H}{c\left(\alpha_1^H+\alpha_2^H+\alpha_3^H\right)}
\end{pmatrix}. \tag{3.59}$$

The eigenvalues given by `mathematica` are

$$\lambda_1 = \pm\, i\sqrt{b_h d_p} \qquad \text{each with multiplicity 1,} \tag{3.60}$$

$$\lambda_2 = \pm\, i\sqrt{b_h d_p}\frac{\sqrt{\alpha_1^H\left(\alpha_1^H-\alpha_2^H\right)+\alpha_2^H\left(\alpha_2^H-\alpha_3^H\right)-\alpha_3^H\left(\alpha_1^H-\alpha_3^H\right)}}{\alpha_1^H+\alpha_2^H+\alpha_3^H} \tag{3.61}$$

each with multiplicity 2.

Assuming $\alpha_1^H > \alpha_2^H > \alpha_3^H$ the term under the square root becomes positive and all eigenvalues have a real part zero. This means neutral stability of the inner fixed point for $n = 3$.

For all models in general, if birth rate of hosts and death rate of parasites are positive, and payoffs are chosen in a logical way, the eigenvalues seem to be purely imaginary or zero which means neutral stability of the fixed point.

3.2 Constant of motion

3.2.1 Replicator dynamics

Matching allele model

Like in the 2 × 2 case [Song et al., 2015; Hofbauer and Sigmund, 1998], a simple constant of motion is obtained.

$$\begin{aligned} H &= \log \prod_{i=1}^{n} p_i + \log \prod_{i=1}^{n} h_i \\ &= \sum_{i=1}^{n} \log p_i + \sum_{i=1}^{n} \log h_i \end{aligned} \tag{3.62}$$

The time derivative is zero, which proves that this is a constant of motion.

$$\begin{aligned} \dot{H} &= \sum_{i=1}^{n} \frac{\dot{p}_i}{p_i} + \sum_{i=1}^{n} \frac{\dot{h}_i}{h_i} \\ &= \underbrace{\sum_{i=1}^{n} h_i}_{=1} - \sum_{i=1}^{n} \sum_{k=1}^{n} h_k p_k - \underbrace{\sum_{i=1}^{n} p_i}_{=1} + \sum_{i=1}^{n} \sum_{k=1}^{n} h_k p_k \end{aligned} \tag{3.63}$$

Since the population number is kept constant the normalisation can be employed here. In this case H becomes maximal when $\frac{dH}{dh_i} = \frac{dH}{dp_i} = 0$ which is the case when$\frac{1}{h_i} + \frac{-1}{1-\sum_{k=1}^{n-1} h_k} = 0$ and $\frac{1}{p_i} + \frac{-1}{1-\sum_{k=1}^{n-1} p_k} = 0$. This means that H reaches its maximum at the inner fixed point $h_i^* = p_i^* = \frac{1}{n}$. For other trajectories (starting with other initial conditions), the constant of motion can be interpreted as the distance from the fixed point. For the 2 × 2 case some constants are visualised in Figure 3.1. The state space is confined to two dimensions, leaving room for a third axis showing the value of the constant of motion. The left axis shows the relative frequencies of host types and the right axis shows frequencies of parasites. Different colours represent different constants, where the darkest at the top is the largest constant and the trajectory is close to the fixed point.

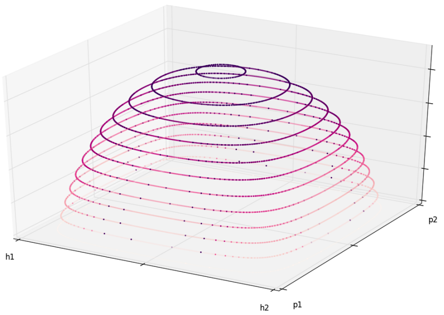

Figure 3.1: Constants of motion for a two type replicator dynamics matching allele model. Left (and right) axis: Host (and parasite) type distribution. Hight/colour intensity: Value of constant of motion

Cross-infection

For this model the same constant of motion was found.

$$H = \log \prod_{i=1}^{n} p_i + \log \prod_{i=1}^{n} h_i$$

The proof is shown in the Appendix in Section 6.2

General infection

A constant of motion was derived for the case $M^H = -cM^P$ with certain restrictions that had to be made (see Appendix 6.2). A more general approach is to assume $M^H = -c \cdot \left(M^P\right)^T$ (Equation 3.36). In [Hofbauer, 1996] a constant of motion is found for the n-dimensional replicator equation. In this case a constant of motion is

$$H = \sum_{i=1}^{n} \log h_i + c \sum_{i=1}^{n} \log p_i \tag{3.64}$$

This is derived in the Appendix in Section 6.2.

3.2.2 Lotka-Volterra

Matching allele model

A constant of motion was discovered similar to Theorem 4.3 in [Plank, 1995].

$$\begin{aligned} H &= \sum_{i=1}^{n} h_i - \sum_{i=1}^{n} h_i^* \log h_i + \sum_{i=1}^{n} p_i - \sum_{i=1}^{n} p_i^* \log p_i \qquad (3.65) \\ &= \sum_{i=1}^{n} h_i - d_p \sum_{i=1}^{n} \log h_i + \sum_{i=1}^{n} p_i - b_h \sum_{i=1}^{n} \log p_i \\ \dot{H} &= \sum_{i=1}^{n} \dot{h}_i - d_p \sum_{i=1}^{n} \frac{\dot{h}_i}{h_i} + \sum_{i=1}^{n} \dot{p}_i - b_h \sum_{i=1}^{n} \frac{\dot{p}_i}{p_i} \qquad (3.66) \\ &= \sum_{i=1}^{n} h_i \left(-p_i + b_h\right) - d_p \sum_{i=1}^{n} \left(-p_i + b_h\right) + \sum_{i=1}^{n} p_i \left(h_i - d_p\right) - b_h \sum_{i=1}^{n} \left(h_i - d_p\right) \\ &= 0 \end{aligned}$$

Note that in the Lotka-Volterra system the fixed point depends on the model so that this time it is indispensable to include it in the constant.

Cross-infection

The same constant of motion is found for the cross infection model

$$H = \sum_{i=1}^{n} h_i - \sum_{i=1}^{n} h_i^* \log h_i + \sum_{i=1}^{n} p_i - \sum_{i=1}^{n} p_i^* \log p_i, \tag{3.67}$$

with the corresponding fixed point

$$H = \sum_{i=1}^{n} h_i - \frac{d_p}{3} \sum_{i=1}^{n} \log h_i + \sum_{i=1}^{n} p_i - \frac{b_h}{3} \sum_{i=1}^{n} \log p_i. \tag{3.68}$$

The time derivation is similar to before

$$\begin{aligned}\dot{H} &= \sum_{i=1}^{n} \dot{h}_i - \frac{d_p}{3} \sum_{i=1}^{n} \frac{\dot{h}_i}{h_i} + \sum_{i=1}^{n} \dot{p}_i - \frac{b_h}{3} \sum_{i=1}^{n} \frac{\dot{p}_i}{p_i} \qquad (3.69)\\ &= \sum_{i=1}^{n} h_i \left(-\left(p_{i-1} + p_i + p_{i+1}\right) + b_h\right) - \frac{d_p}{3} \sum_{i=1}^{n} \left(-\left(p_{i-1} + p_i + p_{i+1}\right) + b_h\right)\\ &\quad + \sum_{i=1}^{n} p_i \left(\left(h_{i-1} + h_i + h_{i+1}\right) - d_p\right) - \frac{b_h}{3} \sum_{i=1}^{n} \left(\left(h_{i-1} + h_i + h_{i+1}\right) - d_p\right)\\ &= 0.\end{aligned}$$

General infection

In [Hofbauer and Sigmund, 1998] (chapter 2) a constant of motion is derived for the two-dimensional Lotka-Volterra equation. This can be extended for n dimensions (see also [Plank, 1995]). It is assumed again that $M^H = -c \cdot \left(M^P\right)^T$.

$$H = \sum_{i=1}^{n} h_i - \sum_{i=1}^{n} h_i^* \log h_i + c * \sum_{i=1}^{n} p_i + c \sum_{i=1}^{n} p_i^* \log p_i \qquad (3.70)$$

Inserting the fixed point and making use of the transposition yields

$$H = \sum_{i=1}^{n} h_i - \frac{d_p}{\sum_k \alpha_k^H} \sum_{i=1}^{n} \log h_i + c \sum_{i=1}^{n} p_i - \frac{b_h}{\sum_k \alpha_k^H} \sum_{i=1}^{n} \log p_i. \qquad (3.71)$$

The time derivation proves the constant

$$\dot{H} = \sum_{i=1}^{n} \dot{h}_i - \frac{d_p}{\sum_k \alpha_k^H} \sum_{i=1}^{n} \frac{\dot{h}_i}{h_i} + c \sum_{i=1}^{n} \dot{p}_i - \frac{b_h}{\sum_k \alpha_k^H} \sum_{i=1}^{n} \frac{\dot{p}_i}{p_i}. \qquad (3.72)$$

After inserting the differential equations and some transformations one gets

$$\begin{aligned}\dot{H} &= b_h \sum_{i=1}^{n} h_i + \frac{c d_p}{\sum_k \alpha_k^H} \sum_{i=1}^{n} \left(\left(M^P\right)^T p\right)_i - c d_p \sum_{i=1}^{n} p_i - \frac{b_h}{\sum_k \alpha_k^H} \sum_{i=1}^{n} \left(M^P h\right)_i \qquad (3.73)\\ &= b_h \sum_{i=1}^{n} h_i + \frac{c d_p}{\sum_k \alpha_k^H} \sum_{k=1}^{n} \sum_{i=1}^{n} \alpha_k^H p_i - c d_p \sum_{i=1}^{n} p_i - \frac{b_h}{\sum_k \alpha_k^H} \sum_{k=1}^{n} \sum_{i=1}^{n} \alpha_k^H h_i\\ &= 0.\end{aligned}$$

Note that for all constants of motions mentioned for Lotka-Volterra dynamics the fixed point plays an important role.

4 Numerical analysis

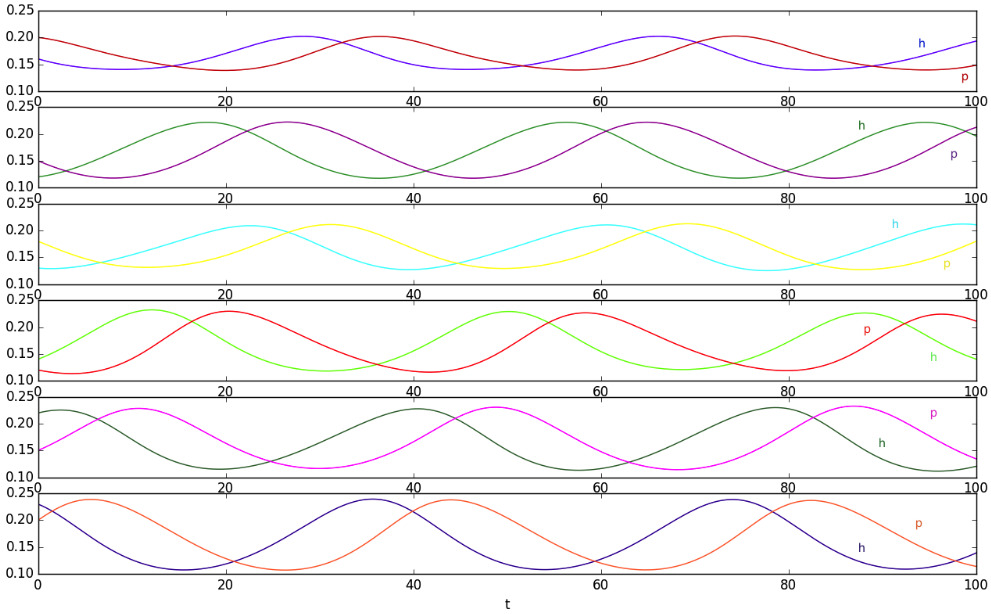

Figure 4.1: **Matching allele replicator dynamics with six types**
Numerical solution for six types of hosts (in blue and green) and parasites (in red and yellow) analysed with replicator dynamics. Initial conditions: $h(0) = [0.16, 0.12, 0.13, 0.14, 0.22, 0.23]^T$ and $p(0) = [0.2, 0.15, 0.18, 0.12, 0.15, 0.2]^T$

A simple example host parasite replicator dynamics with six types can be seen in Figure 4.1. The dynamics become more complex when the initial conditions are chosen further from the inner fixed point.

4.1 Three types and chaos

Replicator dynamics

In [Sato et al., 2002] chaotic behaviour and large positive Lyapunov exponents were found for several initial conditions in a two-person rock-paper-scissors game. This is mathematically closely related to a 3 × 3 replicator dynamics host-parasite system. After reproducing their results we transferred their approach to our matching allele model and analysed several initial conditions $h(0) = [0.5, 0.01k, 0.05 - 0.01k]^T$ and $p(0) = [0.5, 0.25, 0.25]^T$. We saw periodic trajectories for $k = 5 - 25$ in the Poincaré section $h_2 - h_1 + p_2 - p_1 = 0$ (Figure 4.2a) and $\log h_1 h_2 h_3 - \log p_1 p_2 p_3 = 0$ (Figure 4.2b). For initial conditions corresponding to $k = 1, 2, 3, 4$ (black, green, blue and red scatter points, which are not on closed trajectories) there seems to be chaos. Two initial conditions ($k = 1, 10$) were further analysed to differentiate between chaotic and non-chaotic initial conditions. A Fourier spectrum analysis did not lead to clear results since for both initial conditions a small peak in the Fourier spectrum at 0.05 which corresponds

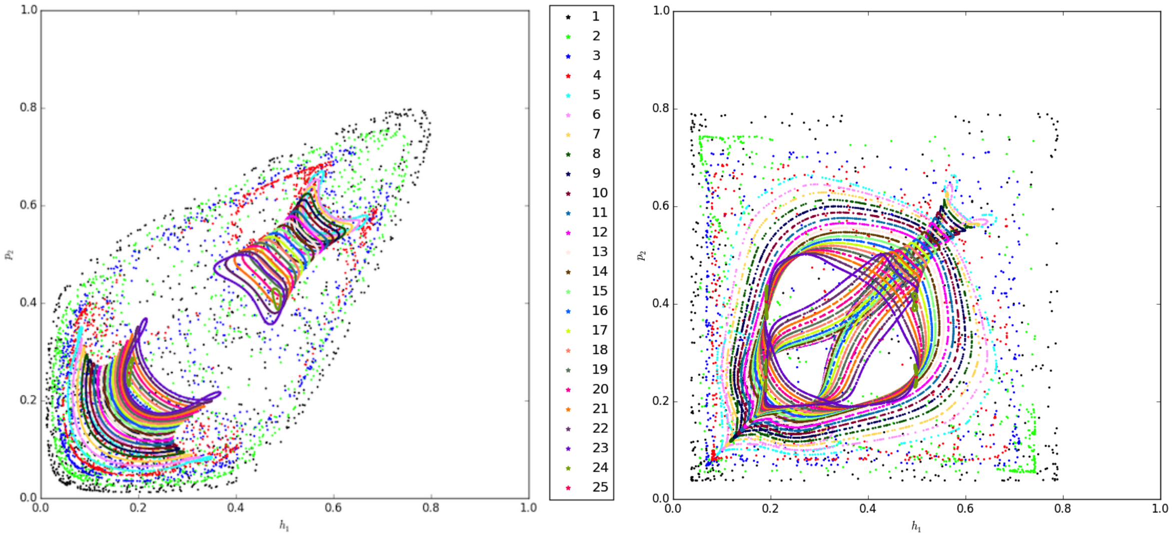

(a) $|h_2 - h_1 + p_2 - p_1| \leq 0.001$

(b) $|\log h_1 h_2 h_3 - \log p_1 p_2 p_3| \leq 0.001$

Figure 4.2: **Matching allele replicator dynamics with three types**
Poincaré sections for a 3-type matching allele replicator dynamics system following method by Sato et al. [2002]. Restrictions see (a) and (b). Plotted in the $h_1 - p_2-$plane. Numerical integration with `python`'s built in `odeint` function. Initial conditions: $h(0) = [0.5, 0.01k, 0.5 - 0.01k]^T$ and $p(0) = [0.5, 0.25, 0.25]^T$ for $k = 1, 2, ..., 25$ (see legend).

to a period of $\frac{2\pi}{0.05} = 128$ showed up. This must not be confused with the oscillation frequency close to the inner fixed point in Equation 3.49.

Plotting trajectories in the state space or, for reduction of dimensionality, on simplices visualises the complexity of the system (see Appendix 6.3). Figure 4.3 shows the numerical solution for a three-type matching allele system analysed with replicator equations. Each of the three corners in plot 4.3a and 4.3b represents one type of host, where the other two types are nonexistent. It becomes clear that for balanced initial conditions corresponding to $k = 10$, close to the center of the simplex, frequencies do not leave the space of the trajectory drawn and are therefore confined to orbits around the inner fixed point. For more extreme initial conditions, starting close to the edge of the simplex in plot (b) $(k = 1)$ this cannot be said. The trajectory is not limited to regular orbits but nearly fills out the whole parameter space, going from conditions close to extinction of one type (edges of simplex) to a near balance of all types (close to the inner fixed point). Figures 4.3c and 4.3d show a three dimensional projection of the four dimensional data received after reducing the dimension to two for each species (see Appendix 6.3). The host simplex and the parasite simplex (which looks exactly the same) are combined in these figures. Three of the dimensions are used to plot the 3D-projection. The colour depicts the fourth dimension. Even after 10 000 generations plotted with a stepsize of 0.1 the trajectory stays on a restricted space for initial condition $k = 10$. Again, the extreme condition $k = 1$ shows a much wider use of the state space and no regularity.

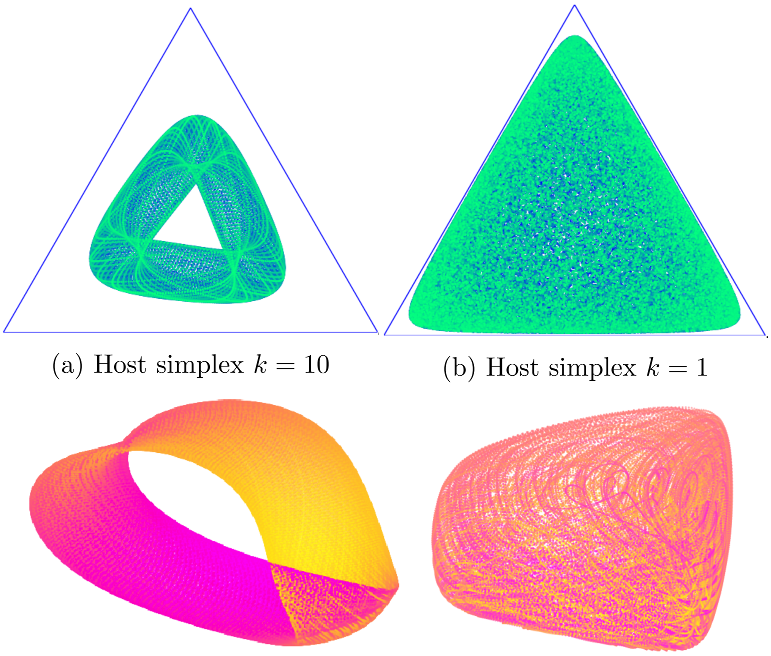

(a) Host simplex $k = 10$

(b) Host simplex $k = 1$

(c) 4D projection $k = 10$

(d) 4D projection $k = 1$

Figure 4.3: **Matching allele replicator dynamics with three types**
Simplices for a 3-type matching allele replicator dynamics system with initial conditions $h\,(0) = [0.5, 0.01k, 0.5 - 0.01k]^T$ and $p\,(0) = [0.5, 0.25, 0.25]^T$, $k = 10$ (left) and $k = 1$ (right). Numerical integration with `python`'s built-in `odeint` function.
(a) and (b): $2D$-simplex for hosts. Each vertex corresponds to a sole existence of one host type. The time is represented by the colour going from blue (generation 0) to green (generation 2000).
(c) and (d): $4D$ data as $3D$-projection. The x- and y-axis represent the $2D$-parasite-simplex. The z-axis represents one axis of the $2D$-host-simplex of (a) and (b), the second axis of the host simplex is represented in the colour change. Trajectories were plotted for 10 000 generations with a stepsize of 0.1.

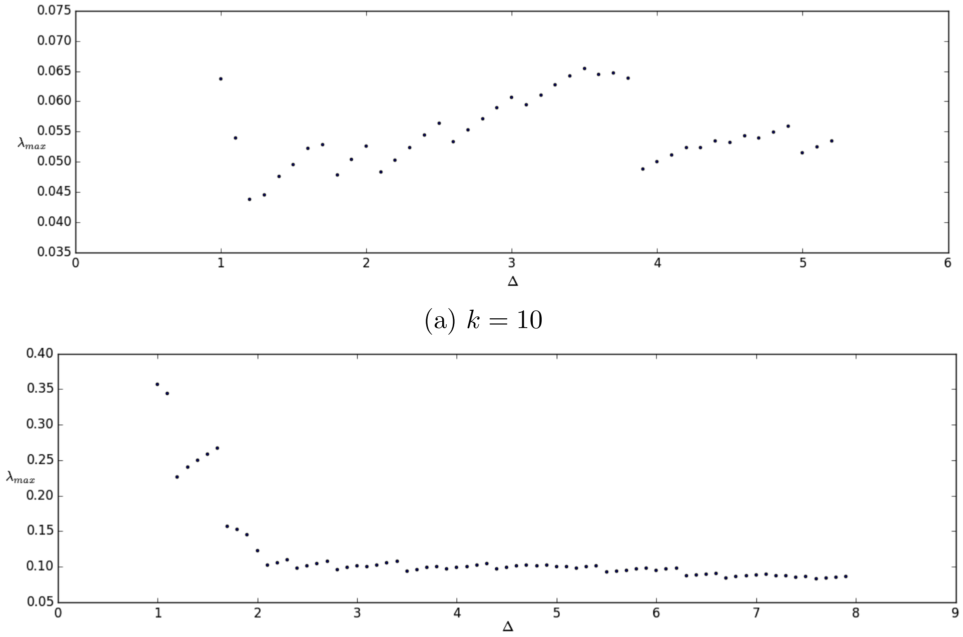

(a) $k = 10$

(b) $k = 1$

Figure 4.4: **Matching allele replicator dynamics with three types** Estimation of the largest Lyapunov exponent $\lambda_{max} = \frac{\Delta}{V(\Delta)}$ for a 3-type matching allele replicator dynamics system using the method of Kim and Choe [2010], with `bigfloat` precision 300 in a fourth-order Runge-Kutta integration. Initial conditions $h(0) = [0.5, 0.1, 0.4]^T$ $(k = 10)$ and $h(0) = [0.5, 0.01, 0.49]^T$ $(k = 1)$, $p(0) = [0.5, 0.25, 0.25]^T$. Initial distance defined by $D = 50$. Maximum 100 generations.

To further strengthen the chaos argument the largest Lyapunov exponent was estimated, after successfully reproducing the results from Kim and Choe [2010] with methods described in Section 2.7 (for `python` code see Appendix 6.3). In Figure 4.4 the estimated Lyapunov exponent for a moderate initial condition $(k = 10)$ is a constant of approximately 0.055 with relatively large variance. For $k = 1$ a much larger value around 0.1 is obtained. This is consistent with the magnitude of estimated values in Kim and Choe [2010].

Lotka-Volterra dynamics

The Lotka-Volterra matching allele model is a system of detached differential equations so that dimensions always reduce to two (because there are two species) independent of the number of types n. Poincaré sections showed no irregular trajectories for Lotka-Volterra dynamics with two types of each species (plots not shown). Since the trajectories are not restricted to a specific parameter space, let alone a simplex, it is not possible to show similar figures as above. However, plotting trajectories in the $h_1 - h_2-$plane lead to complex dynamics even in the case of two types when the equations were coupled through a small payoff for mismatching types. This observation was made independent of the initial conditions. Figure 4.5 shows trajectories of a two-type host-parasite Lotka-Volterra model. If only matching host and parasite interact with each other there is no influence from the separated system of second types and the dynamics are very simple. Trajectories are drawn for initial conditions $h(0) = [0.01k, 1 - 0.01k]^T$ for $k = 1, 2, ..., 25$, while the parasites' initial condition stays constant: $p(0) = [0.5, 0.5]^T$. For each initial condition there is a simple orbits around the inner fixed point in Figure 4.5a. However, adding a small influence of parasite two to host one (one fifth of the payoff for matching types) the picture already looks very different. In Figure 4.5b two initial conditions are shown, $k = 1$

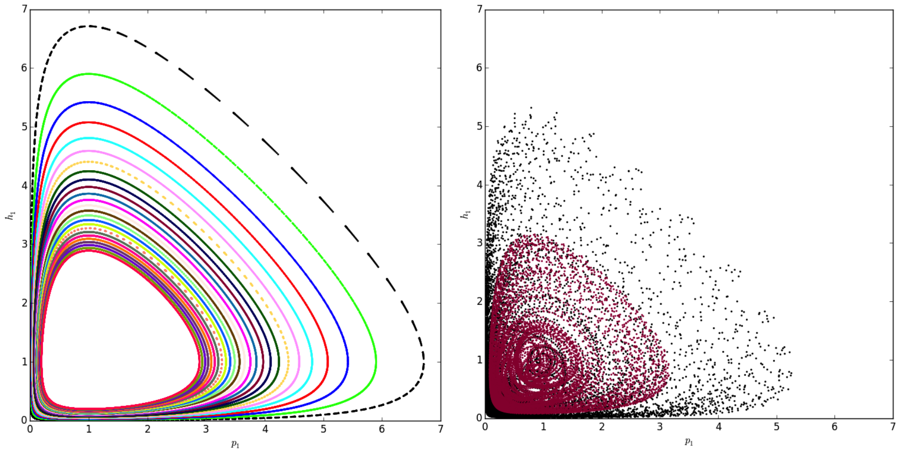

(a) Matching allele

(b) Coupled

Figure 4.5: **General Lotka-Volterra model with two types**
Trajectories of Lotka-Volterra dynamics for a 2-type replicator dynamics system plotted in the $h_1 - h_2-$plane for 1000 generations with a stepsize of 0.1. Initial conditions: $h\left(0\right) = \left[0.01k, 1 - 0.01k\right]^T$ and $p\left(0\right) = \left[0.5, 0.5\right]^T$. Numerical integration with `python`'s built-in `odeint` function. (a): $k = 1, 2, ..., 25$ in a matching allele model. (b): Additional interaction of mismatching hosts and parasites of strength 0.2, $k = 1$ (black) and $k = 10$ (red).

in black and $k = 10$ in red. The dynamics now seem to be far more chaotic.

4.2 Stochastic simulations

Similar to the two-type model presented in [Gokhale et al., 2013] types die out quickly in a stochastic simulation. For a three-type system less extreme starting conditions prolong the time before extinction compared to simulation with unbalanced initial numbers. Also, amplitudes are generally higher in the case of extreme initial conditions. The Figures 4.6 show the scenario for four types of hosts and parasites in a matching allele model. Starting with 250 individuals of each type of host and parasite (Figure 4.6a) increases the chance of survival. The average time over 20 simulations until one type dies out is 12.7 generations. For extreme conditions, starting with 900 hosts of type one and few of the other three types (Figure 4.6b) reduces the average time until extinction to 2.9 generations.

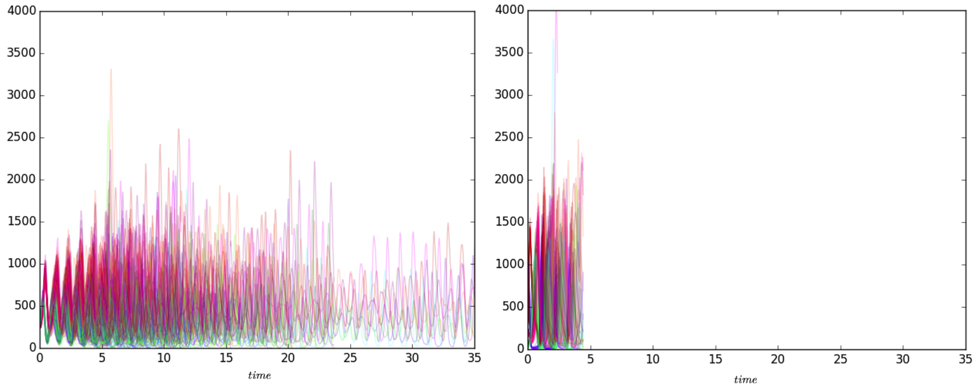

(a) $H(0) = [250, 250, 250, 250]^T$ (b) $H(0) = [900, 50, 25, 25]^T$

Figure 4.6: **Stochastic matching allele model with four types**
20 stochastic simulations as in [Gillespie, 2007] for a 4-type matching allele system, starting with balanced initial conditions (a) and extreme conditions (b) for hosts and $P(0) = [250, 250, 250, 250]^T$ for parasites. $b_h = 5$, $d_p = 2.5$, interaction rate of matching types: $r = 0.01$. Hosts in cold, parasites in warm colours.

5 Discussion

Host and parasite systems with two types of each species have been analysed extensively in deterministic and stochastic models. Hosts and parasites affect each other more than other species due to the intimacy of their relationship. This is why coevolution plays such an important role here.

The classic matching allele and gene-for-gene models are usually in focus when discussing interactions on the genetic level and have even been interpolated to discuss versions in between these two extremes [Agrawal and Lively, 2002]. Several models have shown negative frequency dependent oscillations of host and parasite abundances, named Red Queen dynamics by van Valen [1973]. The Red Queen theory is now a broadly discussed topic and has been empirically strengthened in several field studies [Koskella and Lively, 2009; Decaestecker et al., 2007] and laboratory experiments [Buckling and Rainey, 2002]. A stochastic model with changing population size (Lotka-Volterra) by Gokhale et al. [2013] shows that extinctions were possible, contradicting the Red Queen hypothesis. Song et al. [2015] found that on the gene-for-gene side of the continuum and with changing population size in a deterministic model oscillations become more complex than recently believed. Constants of motion were also presented

In this thesis both models with constant population size (replicator equations) and changing population size (Lotka-Volterra dynamics) were considered. In addition the model was extended to incorporate more than two types of each species which is another step closer to reality. Apart from the matching allele model, the gene-for-gene model and their interpolation, a much wider range of interactions is possible and plausible. One of the aims was to find constant of motions for most complex payoff matrices. They still abide by certain symmetry restrictions (Equation 3.36) but a much wider range of models is now accessible with the tools provided here.

Summary of results

It is not surprising that the inner fixed points of replicator dynamics (Equation 3.1) is $\frac{1}{n}$ for all types, since the frequencies are restricted to the simplex by a constant population size, the nature of replicator dynamics. In the Lotka-Volterra models with changing population size, however, the inner fixed point depends on the birth rates and death rates of host and parasite, respectively (Equations 3.2 - 3.4). The neutral stability of this fixed point, although not in all cases analytically proven, was shown for all reasonable scenarios where one host-parasite pair is dominant (see text after Equation 3.46 for further discussion). Constants of motion were represented for all models in Section 3.2. For replicator dynamics with a uniform fixed point the constant of motion has a simpler form. When Lotka-Volterra dynamics with changing population size is applied the fixed point and, in the most general case, the payoffs play a major role.

Although constants of motions were found for all models, this does not mean that this results in stable trajectories, as was found in Section 4.1. For some initial conditions close to the edge of the simplex chaotic behaviour is possible for replicator dynamics with as little as three types of each species (Figures 4.2, 4.3 and 4.4). For balanced frequencies of host/parasite types there are stable and small oscillations in frequencies of the types. But when initial conditions are further apart the amplitudes become larger. For extreme initial conditions (for example one very frequent type, two very rare types) the system even becomes chaotic. Regular Red Queen dynamics can not be observed under these circumstances. One may admittedly ask the question whether these extreme cases are likely in reality. It is safe to assume though, that for more complex models than the matching allele model the dynamics are not simplified. It is possible that for more complicated payoff matrices the parameter space, where regular orbits are observed, decreases. This was already shown very recently by Rabajante et al. [2015] in purely stochastic models. Since the differential equations are decoupled in a matching allele model with Lotka-Volterra dynamics, it is necessary to link the equations. This was done by allowing a small payoff for mismatching hosts and parasites (see Figure 4.5b). Independent of the initial conditions the trajectories were now more complicated. Finally, the stochastic simulation (Figure 4.6) showed that increasing the number of types still leads to extinction or fixation in models with changing population size.

The results show that already slight diversity (few types or species) and antagonistic mechanisms in systems with simple interactions lead to complex dynamics and chaos. Stable states (fixed points or regular orbits) become more and more unlikely. This suggests that interactions between diverse types of hosts and parasites do not evolve to a stable state or stable oscillations but can persist with chaotic changes of abundances.

Outlook

In the limited time frame of a master thesis project it was not possible to solve to a satisfying extent several problems which arose. It is especially important to find an optimal numerical integrator for such delicate systems which result in chaos. Since the chaotic nature of the system was discovered relatively late in the course of the project it was not possible to go into much detail. An extensive analysis of chaos should be conducted with a better integrator for more complicated replicator dynamic models not just the matching allele model. A focus could lie on Lotka-Volterra dynamics, which were not studied much concerning Lyapunov exponents and Poincaré sections. Roques and Chekroun [2011] suggested that in a Lotka-Volterra system one needs at least four species which interact with each other so as to run into chaos. This could be refined by proving that two species with two types are required for chaos. Apart from Lyapunov exponents a chaos analysis could involve ergodic theory (for analytical work) or time series analysis (concerning numerical results). Concerning the stochastic model, extinction times and extinction probabilities for different types of hosts and parasites could be analysed further under diverse conditions (initial abundances, total population size, reaction rates). Additionally, exploring intra-species interactions for example competition for a common good or cooperative infectivity could be of interest.

Bibliography

Agrawal, A. and Lively, C. M. (2002). Infection genetics: gene-for-gene versus matching-alleles models and all points in between. *Evolutionary Ecology Research*, 4:79–90.

Bell, R. (1996). Ige, allergies and helminth parasites: A new perspective on an old conundrum. *Immunology and Cell Biology*.

Best, A., White, A., and Boots, M. (2009). The implications of coevolutionary dynamics to host-parasite interactions. *The American Naturalist*.

Buckling, A. and Rainey, P. B. (2002). Antagonistic coevolution between a bacterium and a bacteriophage. *Proceedings of the Royal Society B*, 269:931 –936.

Carroll, L. (1871). *Through the Looking-Glass, and What Alice Found There*. Macmillan, London.

Coors, A., Decaestecker, E., Jansen, M., and Meester, L. D. (2008). Pesticide exposure strongly enhances parasite virulence in an invertebrate host model. *Oikos*.

Decaestecker, E., Gaba, S., Raeymaekers, J. A. M., R. Stoks, L. v. K., Ebert, D., and Meester, L. D. (2007). Host–parasite 'red queen' dynamics archived in pond sediment. *Nature*, 450:870–873.

Engelstädter, J. (2015). Host-parasite coevolutionary dynamics with generalized success/failure infection genetics. *The American Naturalist*.

Flor, H. H. (1955). Host-parasite interaction in flax rust - its genetics and other implications. *Phytopathology*, 45:680–685.

Gillespie, D. (2007). Stochastic simulation of chemical kinetics. *Annual Review of Physical Chemistry*, 58:35–55.

Gokhale, C. S., Papkou, A., Traulsen, A., and Schulenburg, H. (2013). Lotka-Volterra dynamics kills the Red Queen: population size fluctuations and associated stochasticity dramatically change host-parasite coevolution. *BMC Evolutionary Biology*, 13:254.

Hamilton, W. D., Axelrodlrod, R., and Tanese, R. (1990). Sexual reproduction as an adaptation to resist parasites (a review). *Proceedings of the National Academy of Sciences*.

Hershey, J. E. and Rao Yarlagadda, R. K. (1986). *Data Transportation and Protection*. Springer US.

Hofbauer, J. (1996). Evolutionary dynamics for bimatrix games: A Hamiltonian system? *Journal of Mathematical Biology*, 34:675–688.

Hofbauer, J. and Sigmund, K. (1998). *Evolutionary Games and Population Dynamics*. Cambridge University Press, Cambridge, UK.

Kim, B. J. and Choe, G. H. (2010). High precision numerical estimation of the largest lyapunov exponent. *Communications in Nonlinear Science and Numerical Simulation*.

Koskella, B. and Lively, C. M. (2009). Evidence for negative frequency-dependent selection during experimental coevolution of a freshwater snail and sterlizing trematode. *Evolution*, 63:2213–2221.

Lambert, A. (2014). Predicting the past: Evolution, fate and mathematics. `http://www.college-de-france.fr/site/en-cirb/Predicting-the-past-Evolution-fate-and-mathematics-Amaury-Lambert.htm`. [Online; accessed 22-July-2015].

Lively, C. M. (2010). A review of red queen models for the persistence of obligate sexual reproduction. *Journal of Heredity*, 101(suppl 1):S13–S20.

McKane, A. J. and Newman, T. J. (2004). Stochastic models in population biology and their deterministic analogs. *Physical Review E*, 70:19.

Nowak, M. A. (2006). *Evolutionary dynamics.* Harvard University Press, Cambridge MA.

Plank, M. (1995). Hamiltonian structures for the n-dimensional lotka-volterra equations. *Journal of Mathematical Physics*, 36(7):3520–3534.

Quigley, B. J. Z., García López, D., Buckling, A., McKane, A. J., and Brown, S. P. (2012). The mode of host-parasite interaction shapes coevolutionary dynamics and the fate of host cooperation. *Proceedings of the Royal Society B: Biological Sciences*, 279(1743):3742–3748.

Rabajante, J. F., Tubay, J. M., Uehara, T., Morita, S., Ebert, D., and Yoshimura, J. (2015). Red queen dynamics in multi-host and multi-parasite interaction systems. *Scientific Reports.*

Roques, L. and Chekroun, M. D. (2011). Probing chaos and biodiversity in a simple competition model. *Ecological Complexity.*

Salathé, M., Kouyos, R., and Bonhoeffer, S. (2008). The state of affairs in the kingdom of the Red Queen. *Trends in Ecology & Evolution*, 23(8):439–445.

Sato, Y., Akiyama, E., and Farmer, J. D. (2002). Chaos in learning a simple two-person game. *Proceedings of the National Academy of Sciences USA*, 99:4748–4751.

Song, Y., Gokhale, C. S., Papkou, A., Schulenburg, H., and Traulsen, A. (2015). Host-parasite coevolution in populations of constant and variable size. *http://biorxiv.org/content/early/2014/12/09/012435.*

Taylor, P. D. and Jonker, L. (1978). Evolutionarily stable strategies and game dynamics. *Mathematical Biosciences*, 40:145–156.

van Rossum, G. (1995). Python tutorial. *CWI Report CS-R9526.*

van Valen, L. (1973). A new evolutionary law. *Evolutionary Theory*, 1:1–30.

Wolfram Research, I. (2014). Mathematica.

Zeeman, E. C. (1980). Population dynamics from game theory. *Lecture Notes in Mathematics*, 819:471–497.

6 Appendix

6.1 Jacobian entries

In Section 3.1 a stability analysis was conducted by evaluating the Jacobian matrix close to the inner fixed point. The number of differential equations was reduced which makes the entries look complicated in the beginning but greatly simplifies the structure of the Jacobian after inserting the fixed point. For the sake of completeness the Jacobian entries are listed here.

6.1.1 Replicator dynamics: matching allele model

$$\frac{\partial \dot{h}_i}{\partial h_i} = -p_i + \sum_{k=1}^{n-1} h_k p_k + \left(1 - \sum_{k=1}^{n-1} h_k\right)\left(1 - \sum_{k=1}^{n-1} p_k\right) + p_i - \left(1 - \sum_{k=1}^{n-1} p_k\right) \tag{6.1}$$

$$\frac{\partial \dot{h}_i}{\partial h_l} = h_i \left(p_l - \left(1 - \sum_{k=1}^{n-1} p_k\right)\right) \tag{6.2}$$

$$\frac{\partial \dot{h}_i}{\partial p_i} = h_i \left(-1 + h_i - \left(1 - \sum_{k=1}^{n-1} h_k\right)\right) \tag{6.3}$$

$$\frac{\partial \dot{h}_i}{\partial p_l} = h_i \left(h_l - \left(1 - \sum_{k=1}^{n-1} h_k\right)\right) \tag{6.4}$$

$$\frac{\partial \dot{p}_i}{\partial h_i} = p_i \left(1 - p_i + \left(1 - \sum_{k=1}^{n-1} p_k\right)\right) \tag{6.5}$$

$$\frac{\partial \dot{p}_i}{\partial h_l} = p_i \left(-p_l + \left(1 - \sum_{k=1}^{n-1} p_k\right)\right) \tag{6.6}$$

$$\frac{\partial \dot{p}_i}{\partial p_i} = h_i - \sum_{k=1}^{n-1} h_k p_k - \left(1 - \sum_{k=1}^{n-1} h_k\right)\left(1 - \sum_{k=1}^{n-1} p_k\right) - h_i + \left(1 - \sum_{k=1}^{n-1} h_k\right) \tag{6.7}$$

$$\frac{\partial \dot{p}_i}{\partial p_l} = p_i \left(-h_l + \left(1 - \sum_{k=1}^{n-1} h_k\right)\right) \tag{6.8}$$

6.1.2 Replicator dynamics: cross-infection

$$
\frac{\partial \dot{h}_1}{\partial h_l} = \begin{cases} -\left(1-\displaystyle\sum_{k=3}^{n-1} p_k\right) + h_1\left(1-\displaystyle\sum_{k=3}^{n-1} p_k\right) + \displaystyle\sum_{k=2}^{n-2} h_k\left(p_{k-1}+p_k+p_{k+1}\right) & \\ \quad +h_{n-1}\left(1-\displaystyle\sum_{k=1}^{n-3} p_k\right) + \left(1-\displaystyle\sum_{k=1}^{n-1} h_k\right)\left(1-\displaystyle\sum_{k=2}^{n-2} p_k\right) & \\ \quad +h_1\left(\left(1-\displaystyle\sum_{k=3}^{n-1} p_k\right)-\left(1-\displaystyle\sum_{k=2}^{n-2} p_k\right)\right) & \text{when } l=1 \\ h_1\left(\left(1-\displaystyle\sum_{k=1}^{n-3} p_k\right)-\left(1-\displaystyle\sum_{k=2}^{n-2} p_k\right)\right) & \text{when } l=n-1 \\ h_1\left(\left(p_{l-1}+p_l+p_{l+1}\right)-\left(1-\displaystyle\sum_{k=2}^{n-2} p_k\right)\right) & \text{else} \end{cases} \tag{6.9}
$$

$$
=0 \qquad \text{for} \quad h_i^* = p_i^* = \frac{1}{n}
$$

for $n-1 \neq i \neq 1$:

$$
\frac{\partial \dot{h}_i}{\partial h_l} = \begin{cases} h_i\left(\left(1-\displaystyle\sum_{k=3}^{n-1} p_k\right)-\left(1-\displaystyle\sum_{k=2}^{n-2} p_k\right)\right) & \text{when } l=1 \\ -\left(p_{i-1}+p_i+p_{i+1}\right) + h_1\left(1-\displaystyle\sum_{k=3}^{n-1} p_k\right) + \displaystyle\sum_{k=2}^{n-2} h_k\left(p_{k-1}+p_k+p_{k+1}\right) & \\ \quad +h_{n-1}\left(1-\displaystyle\sum_{k=1}^{n-3} p_k\right) + \left(1-\displaystyle\sum_{k=1}^{n-1} h_k\right)\left(1-\displaystyle\sum_{k=2}^{n-2} p_k\right) & \\ \quad +h_i\left(p_{i-1}+p_i+p_{i+1}\right)-\left(1-\displaystyle\sum_{k=2}^{n-2} p_k\right) & \text{when } l=i \\ h_i\left(\left(1-\displaystyle\sum_{k=1}^{n-3} p_k\right)-\left(1-\displaystyle\sum_{k=2}^{n-2} p_k\right)\right) & \text{when } l=n-1 \\ h_i\left(p_{l-1}+p_l+p_{l+1}-\left(1-\displaystyle\sum_{k=2}^{n-2} p_k\right)\right) & \text{else} \end{cases} \tag{6.10}
$$

$$
=0 \qquad \text{for} \quad h_i^* = p_i^* = \frac{1}{n}
$$

$$\frac{\partial \dot{h}_{n-1}}{\partial h_l} = \begin{cases} h_{n-1}\left(\left(1-\sum_{k=3}^{n-1} p_k\right)-\left(1-\sum_{k=2}^{n-2} p_k\right)\right) & \text{when } l=1 \\ -\left(1-\sum_{k=1}^{n-3} p_k\right)+h_1\left(1-\sum_{k=3}^{n-1} p_k\right)+\sum_{k=2}^{n-2} h_k\left(p_{k-1}+p_k+p_{k+1}\right) & \\ \quad +h_{n-1}\left(1-\sum_{k=1}^{n-3} p_k\right)+\left(1-\sum_{k=1}^{n-1} h_k\right)\left(1-\sum_{k=2}^{n-2} p_k\right) & \\ \quad +\left(1-\sum_{k=1}^{n-3} p_k\right)-\left(1-\sum_{k=2}^{n-2} p_k\right) & \text{when } l=n-1 \\ h_{n-1}\left(p_{l-1}+p_l+p_{l+1}-\left(1-\sum_{k=2}^{n-2} p_k\right)\right) & \text{else} \end{cases} \tag{6.11}$$

$$=0 \qquad \text{for} \quad h_i^* = p_i^* = \frac{1}{n}$$

$$\frac{\partial \dot{h}_1}{\partial p_l} = \begin{cases} h_1\left(h_2-h_{n-1}\right) & \text{when } l=1 \\ h_1\left(h_2+h_3-\left(1-\sum_{k=1}^{n-1} h_k\right)-h_{n-1}\right) & \text{when } l=2 \\ h_1\left(1-h_1+h_{n-3}+h_{n-2}-\left(1-\sum_{k=1}^{n-1} h_k\right)\right) & \text{when } l=n-2 \\ h_1\left(1-h_1+h_{n-2}\right) & \text{when } l=n-1 \\ h1\left(1-h_1+h_{l-1}+h_l+h_{l+1}-h_{n-1}-\left(1-\sum_{k=1}^{n-1} h_k\right)\right) & \text{else} \end{cases} \tag{6.12}$$

$$= \begin{cases} 0 & \text{when } l \in \{1,2\} \\ \frac{1}{n} & \text{else} \end{cases} \qquad \text{for} \quad h_i^* = p_i^* = \frac{1}{n}$$

$$\frac{\partial \dot{h}_2}{\partial p_l} = \begin{cases} h_2\left(-1+h_2-h_{n-1}\right) & \text{when } l=1 \\ h_2\left(-1+h_2+h_3-h_{n-1}-\left(1-\sum_{k=1}^{n-1} h_k\right)\right) & \text{when } l=2 \\ h_2\left(-1-h_1+h_2+h_3+h_4-h_{n-1}-\left(1-\sum_{k=1}^{n-1} h_k\right)\right) & \text{when } l=3 \\ h_2\left(-h_1+h_{n-3}+h_{n-2}-\left(1-\sum_{k=1}^{n-1} h_k\right)\right) & \text{when } l=n-2 \\ h_2\left(-h_1+h_{n-2}\right) & \text{when } l=n-1 \\ h_2\left(-h_1+h_{l-1}+h_l+h_{l+1}-h_{n-1}-\left(1-\sum_{k=1}^{n-1} h_k\right)\right) & \text{else} \end{cases} \tag{6.13}$$

$$= \begin{cases} -\frac{1}{n} & \text{when } l \in \{1,2,3\} \\ 0 & \text{else} \end{cases} \qquad \text{for} \quad h_i^* = p_i^* = \frac{1}{n}$$

for $i \in \{3, 4, ..., n-3\}$:

$$\frac{\partial \dot{h}_i}{\partial p_l} = \begin{cases} h_i\left(h_2 - h_{n-1}\right) & \text{when } l = 1 \\ h_i\left(h_2 + h_3 - h_{n-1} - \left(1 - \sum_{k=1}^{n-1} h_k\right)\right) & \text{when } l = 2 \\ h_i\left(-h_1 + h_{n-3} + h_{n-2} - \left(1 - \sum_{k=1}^{n-1} h_k\right)\right) & \text{when } l = n-2 \\ h_i\left(-h_1 + h_{n-2}\right) & \text{when } l = n-1 \\ h_i\Bigg(-1 - h_1 + h_{n-4} + h_{n-3} + h_{n-2} & \\ \qquad -h_{n-1} - \left(1 - \sum_{k=1}^{n-1} h_k\right)\Bigg) & \text{when } l \in \{i-1, i, i+1\} \\ h_i\Bigg(-h_1 + h_{n-4} + h_{n-3} + h_{n-2} & \\ \qquad -h_{n-1} - \left(1 - \sum_{k=1}^{n-1} h_k\right)\Bigg) & \text{else} \end{cases} \tag{6.14}$$

$$= \begin{cases} -\frac{1}{n} & \text{when } l \in \{i-1, i, i+1\} \\ 0 & \text{else} \end{cases} \qquad \text{for} \quad h_i^* = p_i^* = \frac{1}{n}$$

$$\frac{\partial \dot{h}_{n-2}}{\partial p_l} = \begin{cases} h_{n-2}\left(h_2 - h_{n-1}\right) & \text{when } l = 1 \\ h_{n-2}\left(h_2 + h_3 - h_{n-1} - \left(1 - \sum_{k=1}^{n-1} h_k\right)\right) & \text{when } l = 2 \\ h_{n-2}\left(-1 - h_1 + h_{n-4} + h_{n-3} + h_{n-2} - \left(1 - \sum_{k=1}^{n-1} h_k\right)\right) & \text{when } l = n-3 \\ h_{n-2}\left(-1 - h_1 + h_{n-3} + h_{n-2} - \left(1 - \sum_{k=1}^{n-1} h_k\right)\right) & \text{when } l = n-2 \\ h_{n-2}\left(-1 - h_1 + h_{n-2}\right) & \text{when } l = n-1 \\ h_{n-2}\left(-h_1 + h_{l-1} + h_l + h_{l+1} - h_{n-1} - \left(1 - \sum_{k=1}^{n-1} h_k\right)\right) & \text{else} \end{cases} \tag{6.15}$$

$$= \begin{cases} -\frac{1}{n} & \text{when } l \in \{n-3, n-2, n-1\} \\ 0 & \text{else} \end{cases} \qquad \text{for} \quad h_i^* = p_i^* = \frac{1}{n}$$

$$\frac{\partial \dot{h}_{n-1}}{\partial p_l} = \begin{cases} h_{n-1}\left(1+h_2-h_{n-1}\right) & \text{when } l=1 \\ h_{n-1}\left(1+h_2+h_3-h_{n-1}-\left(1-\sum_{k=1}^{n-1} h_k\right)\right) & \text{when } l=2 \\ h_{n-1}\left(-h_1+h_{n-3}+h_{n-2}-\left(1-\sum_{k=1}^{n-1} h_k\right)\right) & \text{when } l=n-2 \\ h_{n-1}\left(-h_1+h_{n-2}\right) & \text{when } l=n-1 \\ h_{n-1}\left(1-h_1+h_{l-1}+h_l+h_{l+1}-h_{n-1}-\left(1-\sum_{k=1}^{n-1} h_k\right)\right) & \text{else} \end{cases} \tag{6.16}$$

$$= \begin{cases} 0 & \text{when } l \in \{n-2, n-1\} \\ \frac{1}{n} & \text{else} \end{cases} \qquad \text{for} \quad h_i^* = p_i^* = \frac{1}{n}$$

Similar derivations are achieved for the parasites' differential equations in the lower part of the Jacobian.

6.1.3 Lotka-Volterra: cross-infection

$$\frac{\partial \dot{h}_i}{\partial h_l} = \begin{cases} -\left(p_{i-1}+p_i+p_{i+1}\right)+b_h & \text{when } l=i \\ 0 & \text{else} \end{cases} \tag{6.17}$$

$$=0 \qquad \text{for} \quad h_i^* = \frac{d_p}{3} \text{ and } p_i^* = \frac{b_h}{3}$$

$$\frac{\partial \dot{h}_i}{\partial p_l} = \begin{cases} -h_i & \text{when } l \in \{i-1, i, i+1\} \\ 0 & \text{else} \end{cases} \tag{6.18}$$

$$= \begin{cases} -\frac{d_p}{3} & \text{when } l \in \{i-1, i, i+1\} \\ 0 & \text{else} \end{cases} \qquad \text{for} \quad h_i^* = \frac{d_p}{3} \text{ and } p_i^* = \frac{b_h}{3}$$

$$\frac{\partial \dot{p}_i}{\partial h_l} = \begin{cases} p_i & \text{when } l \in \{i-1, i, i+1\} \\ 0 & \text{else} \end{cases} \tag{6.19}$$

$$= \begin{cases} \frac{b_h}{3} & \text{when } l \in \{i-1, i, i+1\} \\ 0 & \text{else} \end{cases} \qquad \text{for} \quad h_i^* = \frac{d_p}{3} \text{ and } p_i^* = \frac{b_h}{3}$$

$$\frac{\partial \dot{p}_i}{\partial p_l} = \begin{cases} h_{i-1}+h_i+h_{i+1}-d_p & \text{when } l=i \\ 0 & \text{else} \end{cases} \tag{6.20}$$

$$=0 \qquad \text{for} \quad h_i^* = \frac{d_p}{3} \text{ and } p_i^* = \frac{b_h}{3}$$

6.2 Constant of motion

6.2.1 Replicator dynamics: cross-infection

For the replicator dynamics cross-infection model the constant of motion is proven as follows.

$$\begin{aligned}
\dot{H} &= \sum_{i=1}^{n} \frac{\dot{p}_i}{p_i} + \sum_{i=1}^{n} \frac{\dot{h}_i}{h_i} \qquad (6.21)\\
&= \underbrace{\sum_{i=1}^{n} h_{i-1} + h_i + h_{i+1}}_{=3} - \sum_{i=1}^{n}\sum_{k=1}^{n} p_k \left(h_{k-1} + h_k + h_{k+1}\right)\\
&\quad - \underbrace{\sum_{i=1}^{n} p_{i-1} + p_i + p_{i+1}}_{=3} + \sum_{i=1}^{n}\sum_{k=1}^{n} h_k \left(p_{k-1} + p_k + p_{k+1}\right)\\
&= -\sum_{i=1}^{n}\sum_{k=1}^{n} p_k h_{k-1} - \sum_{i=1}^{n}\sum_{k=1}^{n} p_k h_k - \sum_{i=1}^{n}\sum_{k=1}^{n} p_k h_{k+1}\\
&\quad + \sum_{i=1}^{n}\sum_{k=1}^{n} h_k p_{k-1} + \sum_{i=1}^{n}\sum_{k=1}^{n} h_k p_k + \sum_{i=1}^{n}\sum_{k=1}^{n} h_k p_{k+1}
\end{aligned}$$

shifting the index leads to

$$= -n\sum_{k=0}^{n-1} p_{k+1} h_k - n\sum_{k=2}^{n+1} p_{k-1} h_k + n\sum_{k=1}^{n} h_k p_{k-1} + n\sum_{k=1}^{n} h_k p_{k+1}$$

making use of the periodicity ($h_0 = h_n$, etc.) yields

$$\begin{aligned}
&= -n\sum_{k=1}^{n} p_{k+1} h_k - n\sum_{k=1}^{n} p_{k-1} h_k + n\sum_{k=1}^{n} h_k p_{k-1} + n\sum_{k=1}^{n} h_k p_{k+1}\\
&= 0
\end{aligned}$$

6.2.2 Replicator dynamics: general infection

For the most complex replicator dynamics model a constant of motion was derived following Hofbauer [1996] and Plank [1995] where the fixed point is incorporated. Since the fixed point is $\frac{1}{n}$ for each type it does not play a role in the constant and was later neglected (see Section 3.2.1). Here the derivation is shown with the fixed point.

$$
\begin{aligned}
H &= \sum_{i=1}^{n} h_i^* \log h_i + c \sum_{i=1}^{n} p_i^* \log p_i && (6.22)\\
\dot{H} &= \frac{1}{n} \sum_{i=1}^{n} \frac{\dot{h}_i}{h_i} + \frac{c}{n} \sum_{i=1}^{n} \frac{\dot{p}_i}{p_i}\\
&= \frac{1}{n} \sum_{i=1}^{n} \left(\left(M^H p\right)_i - h^T M^H p \right) + \frac{c}{n} \sum_{i=1}^{n} \left(\left(M^P h\right)_i - p^T M^P h \right)\\
&= \frac{1}{n} \sum_{i=1}^{n} \left(\left(-c \left(M^P\right)^T p \right)_i - h^T (-c) \left(M^P\right)^T p \right) + \frac{c}{n} \sum_{i=1}^{n} \left(\left(M^P h\right)_i - p^T M^P h \right)\\
&= \frac{c}{n} \sum_{i=1}^{n} \left(- \left(\left(M^P\right)^T p \right)_i + h^T \left(M^P\right)^T p \right) + \left(\left(M^P h\right)_i - p^T M^P h \right)\\
&= \frac{c}{n} \sum_{i=1}^{n} \left(- \left(\left(p^T M^P\right)^T \right)_i + \left(p^T M^P h\right)^T \right) + \left(\left(M^P h\right)_i - p^T M^P h \right)\\
&= c \left(p^T M^P h\right)^T - c p^T M^P h + \frac{c}{n} \sum_{i=1}^{n} \left(\left(\left(p^T M^P\right)^T \right)_i - \left(M^P h\right)_i \right)\\
&= \frac{c}{n} \sum_{i=1}^{n} \left(\left(\left(p^T M^P\right)^T \right)_i - \left(M^P h\right)_i \right)\\
&= \frac{c}{n} \sum_{i=1}^{n} \left(\left(p^T M^P\right)_i - \left(M^P h\right)_i \right)\\
&= \frac{c}{n} \sum_{i=1}^{n} \left(\alpha_i^H \underbrace{\sum_{k=1}^{n} p_k}_{=1} - \alpha_i^H \underbrace{\sum_{k=1}^{n} h_k}_{=1} \right)\\
&= 0
\end{aligned}
$$

6.2.3 Replicator dynamics: general infection, without assumption

Before it became clear that a symmetry assumption (Equation 3.36) is necessary the following constant of motion was studied.

$$
\begin{aligned}
H &= \sum_{i=1}^{n} \log p_i + c \sum_{i=1}^{n} \log h_i && (6.23)\\
\dot{H} &= \sum_{i=1}^{n} \frac{\partial H}{\partial p_i} \dot{p}_i + \sum_{i=1}^{n} \frac{\partial H}{\partial h_i} \dot{h}_i && (6.24)\\
&= \sum_{i=1}^{n} \frac{\dot{p}_i}{p_i} + c \sum_{i=1}^{n} \frac{\dot{h}_i}{h_i}
\end{aligned}
$$

A constant of motion can be found under the symmetry assumption $M^H = -cM^P$ or $\alpha_i^H = -c\alpha_i^P$ for all $i = 1, 2, ..., n$. Now with $\frac{\dot{p}_i}{p_i} = \left(M^P h\right)_i - p^T M^P h = -c \left(M^H h\right)_i + c p^T M^H h$ and

$\frac{\dot{h}_i}{h_i} = \left(M^H p\right)_i - h^T M^H p$ it follows:

$$\begin{aligned}\dot{H} &= \sum_{i=1}^{n} \left(M^P h\right)_i + c \sum_{i=1}^{n} \left(M^H p\right)_i - np^T M^P h - cnh^T M^H p \\ &= \sum_{i=1}^{n} \alpha_i^H \left(\sum_{k=1}^{n} h_k \right) + c \sum_{i=1}^{N} \alpha_i^P \left(\sum_{k=1}^{n} p_k \right) - Np^T M^P h - cnh^T M^H p \\ &= \sum_{i=1}^{n} -c\alpha_i^P + c \sum_{i=1}^{n} \alpha_i^P - np^T \left(-cM^H\right) h - cnh^T M^H p \\ &= c \left(p^T M^H h - h^T M^H p\right)\end{aligned} \tag{6.25}$$

This is not yet necessarily zero. To understand the terms $p^T M^H h$ and $h^T M^H p$ better we will now look at these sums:

$$\begin{array}{rccccccccccc} p^T M^H h & = & p_1\alpha_1^P h_1 & + & p_1\alpha_2^P h_2 & + & p_1\alpha_3^P h_3 & + & ... & + & p_1\alpha_n^P h_n \\ & + & p_2\alpha_n^P h_1 & + & p_2\alpha_1^P h_2 & + & p_2\alpha_2^P h_3 & + & ... & + & p_2\alpha_{n-1}^P h_n \\ & + & p_3\alpha_{n-1}^P h_1 & + & p_3\alpha_n^P h_2 & + & p_3\alpha_1^P h_3 & + & ... & + & p_3\alpha_{n-2}^P h_n \\ & ... & & & & & & & & & \\ & + & p_n\alpha_2^P h_1 & + & p_n\alpha_3^P h_2 & + & p_n\alpha_4^P h_3 & + & ... & + & p_n\alpha_1^P h_n \end{array} \tag{6.26}$$

and

$$\begin{array}{rccccccccccc} h^T M^H p & = & p_1\alpha_1^P h_1 & + & p_2\alpha_2^P h_1 & + & p_3\alpha_3^P h_1 & + & ... & + & p_n\alpha_n^P h_1 \\ & + & p_1\alpha_n^P h_2 & + & p_2\alpha_1^P h_2 & + & p_3\alpha_2^P h_2 & + & ... & + & p_n\alpha_{n-1}^P h_2 \\ & + & p_1\alpha_{n-1}^P h_3 & + & p_2\alpha_n^P h_3 & + & p_3\alpha_1^P h_3 & + & ... & + & p_n\alpha_{n-2}^P h_3 \\ & ... & & & & & & & & & \\ & + & p_1\alpha_2^P h_n & + & p_2\alpha_3^P h_n & + & p_3\alpha_4^P h_n & + & ... & + & p_n\alpha_1^P h_n \end{array} \tag{6.27}$$

It is easy to see that the difference of these sums is zero if $\alpha_2^P = \alpha_n^P$ and $\alpha_3^P = \alpha_{n-1}^P$ and so on. So that $\alpha_i^P = \alpha_{n-i+2}^P$ for $i = 2, 3, ..., \lceil \frac{n}{2} \rceil$

$$M^H = \begin{pmatrix} \alpha_1^P & \alpha_2^P & \cdots & \alpha_3^P & \alpha_2^P \\ \alpha_2^P & \alpha_1^P & \alpha_2^P & & \alpha_3^P \\ \vdots & \alpha_2^P & \alpha_1^P & \ddots & \vdots \\ \alpha_3^P & & \ddots & \ddots & \alpha_2^P \\ \alpha_2^P & \alpha_3^P & \cdots & \alpha_2^P & \alpha_1^P \end{pmatrix} \tag{6.28}$$

This seems to be the most general payoff matrix for which a constant of motion (of this form) can be found if the necessary condition of transposition (see Section 3.2.1) is not made. Note that this matrix is identical to its transposed form: $M^H = \left(M^H\right)^T$ which makes the model less general than the one shown in the results Section.

6.3 Numerical methods

6.3.1 Simplices

The following setup was used for analysing the three-types replicator equation which lead to results used in Figure 4.3.

```
a=-1. # main diagonal
b=0. # second diagonal
e=0. # third diagonal
mh=np.array([[a,b,e],[e,a,b],[b,e,a]]) # payoff matrix
c=1. # scaling mp
k=1 # for initial condition
h0=np.array([0.5,0.01*k,0.5-0.01*k]) # initial conditions
p0=np.array([0.5,0.25,0.25])
generations=10000.
steps=100000.
n=len(h0)
mp=-c*mh
```

Integration step with `python`'s built in `odeint`:

```
def deriv(y,t): # define differential equations
    h=y[:n] # host frequencies
    p=y[n:]
    h[n-1]=1-sum(h[:n-1]) # normalisation
    p[n-1]=1-sum(p[:n-1])
    dH=np.dot(mh,p) # replicator dynamica
    bh=np.dot(dH,h) # average fitness
    hdot=h*(dH-bh) # ode
    bP=np.dot(mp,h)
    dp=np.dot(bP,p)
    pdot=p*(bP-dp)
    return np.concatenate([hdot,pdot])
time = np.linspace(0.0,generations,steps) # start,end,steps
y = odeint(deriv,np.concatenate([h0,p0]),time) # actual integration
h=y[:,:n]
p=y[:,n:]
```

The following shows how the projection onto the 2-dimensional simplex was done

```
proj=np.array([[-math.cos(30./360.*2.*math.pi), # projection matrix
    math.cos(30./360.*2.*math.pi),0.],
    [-math.sin(30./360.*2.*math.pi),
    -math.sin(30./360.*2.*math.pi),1.]])
[hx,hy] = np.array(np.mat(proj)*np.mat(h.T)) # projection of hosts
[px,py] = np.array(np.mat(proj)*np.mat(p.T))
```

For the two-dimensional simplices hx and hy were plotted in one plot and px and py in another. The four-dimensional plot was done by plotting px, py, and hy, while hx was used for the colour gradient.

6.3.2 Lyapunov exponents

Plots from Kim and Choe [2010] were partly reproduced using the `bigfloat` package in `python`. This was done mostly to verify our code and precision. Initial variables were

```
p=1000
with precision(p):
    D=BigFloat('50') # measure for closeness of initial condition
    Dint=50 # for label
    d=D+BigFloat(’1e-200’) # for distance of initial conditions
    k=BigFloat(’1’) # initial condition
# N: distance measure for trajectories after time t
    Deltamin=BigFloat(’10’) # minimum Delta
    Deltamax=2*D # maximum Delta
    Deltastep=BigFloat(’1’)
    generations=BigFloat(’200’) #maximum timepoint
    generationsint=200. #for linspace (same as generations)
    steps=BigFloat(’2000’) # number of points to be calculated
    stepsint=2000. #for linspace (same as steps)
    step=generations/steps
    t=BigFloat(’0’) #start
    plotmin=BigFloat(’0’) # trajectories plotted from
    plotmax=BigFloat(’100’)/step # trajectories plotted until
```

To check for initial closeness the following was included

```
    devi=10.**(-d)  #difference between initial conditions
    x1=BigFloat(’0’)
    x2=BigFloat(’0.01’)
    x0_a=np.array([x1,x2*k,x1]) # first initial condition
    x0_b=np.array([x1,x2*k+devi,x1]) # second initial condition
        #choose D so that this holds: (change d)
    if (sum((x0_a-x0_b)*(x0_a-x0_b))==0): # maybe low precision
       sys.exit(’Initial conditions are identical’)
    if (log(sum((x0_a-x0_b)*(x0_a-x0_b))**(1./2.))/log(10.)>-D):
        sys.exit(’Please choose closer initial conditions (higher d)’)
```

The vector w will later contain all values of x, y and z for all time points. For example starting in initial condition a

```
    w0=np.array([BigFloat(’0’),BigFloat(’0’),BigFloat(’0’)])
    w=np.vstack([x0_a,w0])
    while len(w)<steps:
        w=np.vstack([w,w0]) #shape(w)=(steps,3)
```

The actual integration is done through a fourth-order Runge-Kutta algorithm using `bigfloat` numbers.

```
for j in np.arange(1,steps): # index of timepoint
    with precision(p):
        def f(t,m):  # differential equations
            s=BigFloat(’10’)
            r=BigFloat(’28’)
            b=BigFloat(’8’)/BigFloat(’3’)
            return [[-s*(w[t,0]+m[0])+s*(w[t,1]+m[1])],
                     [-(w[t,0]+m[0])*(w[t,2]+m[2])+r*(w[t,0]+m[0])],
                     [(w[t,0]+m[0])*(w[t,1]+m[1])-b*(w[t,2]+m[2])]]
        k1=np.array(f(j-1,[0.,0.,0.]))*step # Runge-Kutta k1
        k1.shape=(3,) # reshape
        k2=np.array(f(j-1,k1/BigFloat(’2’)))*step # Runge-Kutta k2
        k2.shape=(3,) # reshape
        k3=np.array(f(j-1,k2/BigFloat(’2’)))*step # Runge-Kutta k3
        k3.shape=(3,) # reshape
        k4=np.array(f(j-1,k3))*step # Runge-Kutta k4
        k4.shape=(3,) # reshape
        kr=(k1+BigFloat(’2’)*(k2+k3)+k4)/BigFloat(’6’) # Runge-Kutta k
        kr.shape=(3,) # reshape
        w[j,:]=w[j-1,:]+kr # update values of next timepoint
w_a=w # matrix contains values for x, y and z for all timepoints
      # starting with initial condition x0_a
```

The same procedure is used for initial condition b. Now the larges Lyapunov exponent is estimated.

```
with precision(p):
    t = np.linspace(0.,generationsint,stepsint+1)
    Delta=np.arange(Deltamin,Deltamax,Deltastep)
    V=zeros(len(Delta))
    for Deltarun in range(len(Delta)):
      z=np.array([(sum(((w_a-w_b)*(w_a-w_b)),axis=1))
                     **(BigFloat(’1’)/BigFloat(’2’))])>=BigFloat(’10’)
                     **((-D+N[Deltarun]))   # z is a boolean which is
    # True if the trajectories are further apart than the parameter
    # Delta allows
      z.shape=(steps,)
      exist=t[z]
      if len(exist)>BigFloat(’0’):
            V[Deltarun]=exist[0] # minimum time point
      else:
            V[Deltarun]=float(’nan’) # not existent
    G=Delta/V   # approximates lambda_max
```

The same procedure of estimating the largest Lyapunov exponent was applied to the host-parasite matching allele model with replicator equations. Initial conditions were chosen as for the Poincaré sections.

```
    d=D+log(2.)/log(10.) # for distance of initial conditions
    devi=10.**(-d)  # half difference between initial conditions
    x1=BigFloat(’0.5’)
    x2=BigFloat(’0.01’)
    x3=BigFloat(’0.25’)
    x0_a=np.array([x1,x2*k,x1-x2*k,x1,x3,x3]) #h0,p0 (a)
    x0_b=np.array([x1,x2*k+devi,x1-x2*k-devi,x1,x3,x3]) # h0,p0 (b)
```

Differential equations:

```
with precision(p):
    def f(t,m):
        w[t,:]=w[t,:]+m  # timepoint t, m for Runge-Kutta update
        h=w[t,:3]
        p=w[t,3:]
        avrg=h[0]*p[0]+h[1]*p[1]+h[2]*p[2]
        return [h[0]*(-p[0]+avrg),h[1]*(-p[1]+avrg),h[2]*(-p[2]+avrg),
        p[0]*(h[0]-avrg),p[1]*(h[1]-avrg),p[2]*(h[2]-avrg)]
```

6.3.3 Stochastic simulations

Implementation of the Gillespie stochastic simulation algorithm described in Section 2.8 is shown here for a matching allele model with three types.
Setup:

```
nspec=6 #number of types of both species
bound=1000. # number of individuals of each species
runs=10 # number of runs 10
k=1
bh=5. # birth host rate    h1 -> h1+h1 / h2 -> h2+h2
dp=2.5 # death parasite rate p1 -> E / p2 -> E
r1=10./bound # interaction rate of h1 and p1  h1+p1 -> p1+p1
r2=10./bound # interaction rate of h2 and p2  h2+p2 -> p2+p2
r3=10./bound
h01=0.50*bound #initial number of types
h02=0.01*k*bound
```

```
h03=(0.5-0.01*k)*bound
p01=0.50*bound
p02=0.25*bound
p03=0.25*bound
```

The following loop was executed until one type of either species died out.

```
#eventprobabilities without randomness:
prob=np.array([h1*bh,h2*bh,h3*bh,p1*dp,p2*dp,p3*dp,
               h1*p1*r1,h2*p2*r2,h3*p3*r3])
times=[[] for x in xrange(len(prob))] # to store times

for i in np.arange(len(prob)): #for all possible events
    if prob[i]==0: #no changes if species=0 or rate 0
        times[i]='nan'
    else: # time until event
        times[i]=1/prob[i]*np.log(1/np.random.rand(1))
delta_t = min(times) #first event
pos = np.nanargmin(times) # find position of first event
# possible events:
if pos==0:
    h1=h1+1
if pos==1:
    h2=h2+1
if pos==2:
    h3=h3+1
if pos==3:
    p1=p1-1
if pos==4:
    p2=p2-1
if pos==5:
    p3=p3-1
if pos==6:
    p1=p1+1
    h1=h1-1
if pos==7:
    p2=p2+1
    h2=h2-1
if pos==8:
    p3=p3+1
    h3=h3-1
```